Two-electron self-energy corrections to the $2p_{1/2}$-$2s$ transition energy in Li-like ions

V. A. Yerokhin,[1,2] A. N. Artemyev,[1,3] T. Beier,[4] G. Plunien,[5] V. M. Shabaev,[3,6] and G. Soff[5]
[1]*Max-Planck-Institut für Physik komplexer Systeme, Nöthnitzer Straße 38, D-01187 Dresden, Germany*
[2]*Institute for High Performance Computing and Data Bases, Fontanka 118, St. Petersburg 198005, Russia*
[3]*Department of Physics, St. Petersburg State University, Oulianovskaya 1, Petrodvorets, St. Petersburg 198904, Russia*
[4]*Fysik och Teknisk Fysik, Chalmers Tekniska Högskola och Göteborgs Universitet, SE-412 96 Göteborg, Sweden*
[5]*Institut für Theoretische Physik, TU Dresden, Mommsenstraße 13, D-01062 Dresden, Germany*
[6]*GSI, Postfach 11 05 52, D-64223 Darmstadt, Germany*
(Received 29 April 1999)

We present *ab initio* calculations of the complete gauge invariant set of the self-energy screening diagrams for the $2p_{1/2}$-$2s$ transition in Li-like ions. The calculation was performed for extended nuclei in the range $Z=18-100$. Various contributions to the transition energy are collected. The accuracy of theoretical predictions is discussed. [S1050-2947(99)00110-9]

PACS number(s): 31.30.Jv, 31.10.+z

INTRODUCTION

Recent precision measurements in highly charged ions have initiated accurate calculations of energy levels in these systems. Compared to other experimental studies, a measurement of the Lamb shift in high-Z Li-like ions appears to be most promising for testing QED up to second order in α. The uncertainty of the best experimental results for the energy of $2p_{1/2}$-$2s$ the transition in Li-like uranium [1] and the $2p_{3/2}-2s$ transition in Li-like bismuth [2] is by an order of magnitude smaller than the second-order QED contribution to the transition energy. The existing theoretical predictions for transition energies in Li-like ions were obtained using the relativistic many-body perturbation theory [3–5], the multiconfiguration Dirac-Fock method [6], and the configuration-interaction method [7]. All these calculations include second-order QED effects only either phenomenologically, or partly. While these results are in good agreement with the experiment, the full QED calculation to all orders in αZ is still needed. The important role of the second-order QED effects was demonstrated for heliumlike ions in Refs. [8,9], where the two-electron part of the ground-state energy was evaluated taking into account the complete gauge invariant sets of the self-energy and vacuum-polarization screening diagrams.

First steps towards the evaluation of the complete set of the second-order two-electron diagrams for $2p_{1/2}$-$2s$ and $2p_{3/2}$-$2s$ transitions were recently performed in Ref. [10], where the two-electron self-energy correction was calculated for the ground state, and in Ref. [11], where the two-electron vacuum polarization was evaluated for low-lying states of Li-like ions. Preliminary results for the two-electron self-energy and vacuum-polarization corrections for the $2p_{1/2}$-$2s$ transition energy in $^{238}U^{89+}$ were published in Refs. [12,13]. In this paper we present a detailed description of the theoretical and the numerical procedure for the evaluation of the two-electron self-energy corrections for $(1s)^2 2s$ and $(1s)^2 2p_{1/2}$ states of Li-like ions. The method of the computation is based on the numerical procedure developed in Ref. [14] for the first-order self-energy correction. We will, therefore, discuss here only new features of the calculation and refer to that paper for common details.

The paper is organized as follows. In the first section we derive basic formulas using the method of the two-time Green function and discuss the renormalization scheme. In the next section we demonstrate a technique of the evaluation of angular integrals and write formulas in the form suitable for numerical calculation. In the third section we discuss numerical details and present results of the calculation. In the fourth section we collect all contributions to the $2p_{1/2}$-$2s$ transition energy in Li-like ions available at the moment. The theoretical results are compared with experimental data and the accuracy of theoretical predictions is discussed.

Relativistic units are used in this article ($\hbar=c=m=1$). We use roman style (p) for four vectors, boldface (**p**) for three vectors, and italic style (p) for scalars. Four vectors have the form $\mathrm{p}=(\mathrm{p}_0,\mathbf{p})$. The scalar product of two four vectors is $(\mathrm{p}\cdot\mathrm{k})=\mathrm{p}_0\mathrm{k}_0-(\mathbf{p}\cdot\mathbf{k})$. We also use the notations $\not{\mathrm{p}}=\mathrm{p}_\mu\gamma^\mu$, $\hat{\mathbf{p}}=\mathbf{p}/|\mathbf{p}|$.

I. DERIVATION OF BASIC FORMULAS

Our derivation of formulas is based on the method of the two-time Green function developed in Ref. [15]. In the following we give only its brief outline needed for further evaluation. For a detailed description of the method we refer to Refs. [16,17].

The standard definition of the Green function of an N-electron system within QED is

$$G(\mathrm{x}_1',\ldots,\mathrm{x}_N';\mathrm{x}_1,\ldots,\mathrm{x}_N) = \langle 0|T\psi(\mathrm{x}_1')\cdots\psi(\mathrm{x}_N')\overline{\psi}(\mathrm{x}_N)\cdots\overline{\psi}(\mathrm{x}_1)|0\rangle, \quad (1)$$

where $\psi(\mathrm{x})$ is the operator of the electron-positron field in the Heisenberg representation (the Furry picture is assumed), T denotes the time-ordered product and $\overline{\psi}=\psi^\dagger\gamma^0$. The Green function is constructed by perturbation theory using Wick's theorem after the transformation to the interaction picture. To find energy levels of the system, it is more convenient to use the *two-time* Green function

$$G(t_1'=t_2'=\cdots=t_N'\equiv t';t_1=t_2=\cdots=t_N\equiv t). \quad (2)$$

Let us introduce the time-Fourier transform of the two-time Green function by

$$g(E)\,\delta(E-E') = \frac{1}{2\pi i}\,\frac{1}{N!}\int_{-\infty}^{\infty} dt\,dt'\,\exp(iE't'-iEt) \times\langle 0|T\psi(t',\mathbf{x}'_1)\cdots\psi(t',\mathbf{x}'_N) \times\psi^{\dagger}(t,\mathbf{x}_N)\cdots\psi^{\dagger}(t,\mathbf{x}_1)|0\rangle. \tag{3}$$

From the spectral representation of $g(E)$ one can deduce that the two-time Green function has poles at points corresponding to the exact energy levels of the system. Therefore, although the number of variables is considerably reduced in the two-time Green function, it still contains the full information on the energy levels of the system.

Consider now how to extract the energy of a single level of an N-electron system from $g(E)$. We are interested in the energy shift $\Delta E_n = E_n - E_n^{(0)}$ caused by the interaction with the quantized electromagnetic field. Here $E_n^{(0)}$ denotes the unperturbed energy that is the sum of the one-electron Dirac energies, $E_n^{(0)} = \epsilon_1 + \epsilon_2 + \cdots \epsilon_N$ with $(\boldsymbol{\alpha}\mathbf{p} + \beta m + V_c)\psi_k = \epsilon_k \psi_k$. The energy shift ΔE_n of an isolated level due to the interaction with the quantized electromagnetic field is given by [15]

$$\Delta E_n = \frac{(2\pi i)^{-1}\oint_\Gamma dE\;\Delta E\;\Delta g_{nn}(E)}{1+(2\pi i)^{-1}\oint_\Gamma dE\;\Delta g_{nn}(E)}, \tag{4}$$

where the contour Γ surrounds only the unperturbed level $E = E_n^{(0)}$ and is oriented anticlockwise, $\Delta E = E - E_n^{(0)}$, $\Delta g_{nn}(E) = g_{nn}(E) - g_{nn}^{(0)}(E)$, $g_{nn}(E) = \langle u_n|g(E)|u_n\rangle$, u_n is the unperturbed wave function, $g_{nn}^{(0)}(E)$ denotes the $g_{nn}(E)$ function in the zeroth approximation, and $g_{nn}^{(0)}(E) = (E - E_n^{(0)})^{-1}$. By expanding both the numerator and the denominator in Eq. (4) as a standard power series in α, an expansion into energy corrections of different orders is obtained. We write the α expansion of the Green function $g(E)$ as

$$g(E) = g^{(0)}(E) + g^{(1)}(E) + g^{(2)}(E) + \cdots, \tag{5}$$

where the superscript indicates the order in α. For the second-order correction we have

$$\Delta E_n^{(2)} = \frac{1}{2\pi i}\oint_\Gamma dE\;\Delta E\;\Delta g_{nn}^{(2)}(E) - \frac{1}{2\pi i}\oint_\Gamma dE\;\Delta E\;\Delta g_{nn}^{(1)}(E)\,\frac{1}{2\pi i}\oint_\Gamma dE'\,\Delta g_{nn}^{(1)}(E'). \tag{6}$$

For practical calculations it is convenient to express $g_{nn}(E)$ as

$$g_{nn}(E)\,\delta(E-E') = \frac{2\pi}{i}\,\frac{1}{N!}\int_{-\infty}^{\infty} d\mathrm{p}_1^0\cdots d\mathrm{p}_N^0\,d\mathrm{p}_1'^0\cdots d\mathrm{p}_N'^0 \times\delta(E-\mathrm{p}_1^0-\cdots-\mathrm{p}_N^0) \times\delta(E'-\mathrm{p}_1'^0-\cdots-\mathrm{p}_N'^0) \times\langle u_n|G(\mathrm{p}_1'^0,\ldots,\mathrm{p}_N'^0;\mathrm{p}_1^0,\ldots,\mathrm{p}_N^0) \times\gamma_1^0,\ldots,\gamma_N^0|u_n\rangle, \tag{7}$$

where $G(\mathrm{p}_1'^0,\ldots,\mathrm{p}_N'^0;\mathrm{p}_1^0,\ldots,\mathrm{p}_N^0)$ is Green function (1) in the mixed energy-coordinate representation,

$$G(\mathrm{p}_1'^0,\ldots,\mathrm{p}_N'^0;\mathrm{p}_1^0,\ldots,\mathrm{p}_N^0) = (2\pi)^{-2N}\int_{-\infty}^{\infty} d\mathrm{x}_1^0\cdots d\mathrm{x}_N^0\,d\mathrm{x}_1'^0\cdots d\mathrm{x}_N'^0 \times\exp(i\mathrm{p}_1'^0\mathrm{x}_1'^0+\cdots+i\mathrm{p}_N'^0\mathrm{x}_N'^0-i\mathrm{p}_1^0\mathrm{x}_1^0-\cdots-i\mathrm{p}_N^0\mathrm{x}_N^0) \times G(\mathrm{x}'_1,\ldots,\mathrm{x}'_N;\mathrm{x}_1,\ldots,\mathrm{x}_N). \tag{8}$$

Feynman rules for the Green function $G(\mathrm{p}_1'^0,\ldots,\mathrm{p}_N'^0;\mathrm{p}_1^0,\ldots,\mathrm{p}_N^0)$ can be found in Ref. [16].

Let us consider now the two-electron self-energy corrections for the $(1s)^2 2s$ and $(1s)^2 2p_{1/2}$ states of Li-like ions. The unperturbed wave function of a Li-like ion with one electron beyond the closed $(1s)^2$ shell is

$$u_n = \frac{1}{\sqrt{3!}}\sum_P (-1)^P \psi_{1s\uparrow}(P1)\,\psi_{1s\downarrow}(P2)\,\psi_v(P3), \tag{9}$$

where P is the permutation operator and v denotes the valence electron. In this paper we are interested only in two-electron corrections. In this case the three-electron problem can be easily decomposed into three two-electron problems. The two electrons in the $(1s)^2$ shell are equivalent and we have only two different corrections for each state: (i) the δE_{1s}^{1s} correction representing the interaction between two electrons in the closed $(1s)^2$ shell and (ii) the $\delta E_v^{(1s)}$ correction representing the interaction between the valence electron $(v = 2s, 2p_{1/2})$ and the $(1s)^2$ shell.

Let us consider the derivation of basic formulas for a second-order two-electron self-energy correction δE_a^b representing the interaction of electrons in the states a and b. The general formulas can be easily adopted for the corrections

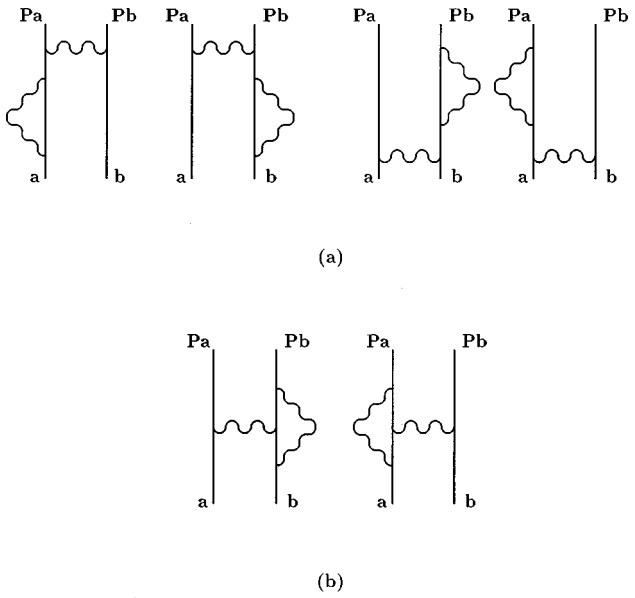

FIG. 1. Two-electron self-energy diagrams for the δE_a^b correction. P denotes the permutation operator.

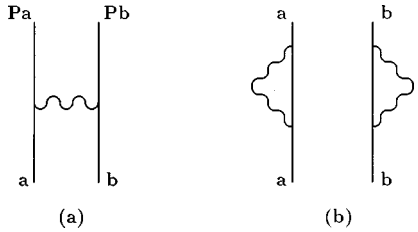

FIG. 2. First-order diagrams contributing to $\Delta g^{(1)}_{nn}$ in Eq. (6) for the δE^b_a correction.

considered here: δE^{1s}_{1s}, δE^{1s}_{2s} ($\delta E^{(1s)}_{2s}=\Sigma_{\mu_{1s}}\delta E^{1s}_{2s}$), and $\delta E^{1s}_{2p}(\delta E^{(1s)}_{2p}=\Sigma_{\mu_{1s}}\delta E^{1s}_{2p}$, μ_{1s} is the magnetic quantum number of an electron in a $1s$ state). In our case, it is sufficient to assume the unperturbed wave function to be represented by the one-determinant two-electron wave function

$$u_n=\frac{1}{\sqrt{2}}\sum_P (-1)^P\psi_{Pa}(\mathbf{x}_1)\psi_{Pb}(\mathbf{x}_2). \tag{10}$$

The derivation for the general case of states with definite angular momentum can be performed in the same way.

The energy shift of an isolated level in second order in α is given by expression (6). For the δE^b_a correction considered here $E^{(0)}_n=\epsilon_a+\epsilon_b$, diagrams contributing to $\Delta g^{(2)}_{nn}$ are shown in Fig. 1, and those contributing to $\Delta g^{(1)}_{nn}$ are shown in Fig. 2. We divide the δE^b_a correction into three parts. The contribution of the diagrams presented in Fig. 1(b) is referred to as *vertex* term ($\Delta E_{\rm ver}$). The contribution of the diagrams in Fig. 1(a) is divided into *reducible* and *irreducible* terms ($\Delta E_{\rm red}$ and $\Delta E_{\rm ir}$, respectively). The reducible part is defined by Fig. 3 and the irreducible part is the remainder. The second term in Eq. (6) is calculated together with the reducible part. Thus, we have

$$\delta E^b_a=\Delta E_{\rm ir}+\Delta E_{\rm ver}+\Delta E_{\rm red}. \tag{11}$$

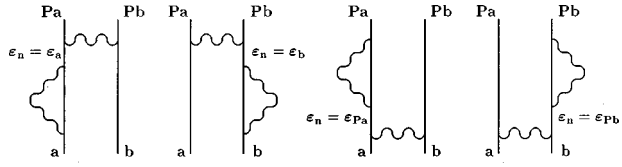

FIG. 3. The reducible part of the two-electron self-energy diagrams. The index n corresponds to intermediate states.

To simplify further the evaluation, we introduce the operator

$$I(\omega)=e^2\alpha^\mu\alpha^\nu D_{\mu\nu}(\omega), \tag{12}$$

where $\alpha^\mu=(1,\boldsymbol{\alpha})$ are the Dirac matrixes, and $D_{\mu\nu}(\omega)$ is the photon propagator. In this paper we work in the Feynman gauge; thus, the photon propagator can be written as

$$D_{\mu\nu}(\omega,\mathbf{x}_{12})=g_{\mu\nu}\frac{\exp[i\sqrt{\omega^2-\mu^2+i\delta}|\mathbf{x}_{12}|]}{4\pi|\mathbf{x}_{12}|}, \tag{13}$$

where $\mathbf{x}_{12}=\mathbf{x}_1-\mathbf{x}_2$, the branch of the square root is fixed by the condition $\mathrm{Im}(\sqrt{\omega^2-\mu^2+i\delta})>0$, δ is small and positive, and μ is the photon mass that is introduced to handle the infrared singularities on intermediate stages of the calculation. We introduce also the self-energy operator $\Sigma(\epsilon)$,

$$\langle a|\Sigma(\epsilon)|b\rangle=\frac{i}{2\pi}\int_{-\infty}^{\infty}d\omega\sum_n\frac{\langle an|I(\omega)|nb\rangle}{\epsilon-\omega-\epsilon_n(1-i0)}, \tag{14}$$

where the summation is carried out over the whole spectrum of the Dirac equation.

A. Irreducible contribution

According to Eqs. (6) and (7), and the Feynman rules for $G(\mathrm{p}_1'^0,\mathrm{p}_2'^0;\mathrm{p}_1^0,\mathrm{p}_2^0)$, we have

$$\begin{aligned}\Delta E_{ir}=\frac{1}{2\pi i}\oint_\Gamma dE\,\Delta E\left(\frac{i}{2\pi}\right)^2\sum_P(-1)^P\int_{-\infty}^{\infty}d\mathrm{p}_1^0\,d\mathrm{p}_1'^0\\
\times\frac{1}{(\mathrm{p}_1'^0-\epsilon_{Pa}+i0)(E-\mathrm{p}_1'^0-\epsilon_{Pb}+i0)}\,\frac{1}{(\mathrm{p}_1^0-\epsilon_a+i0)(E-\mathrm{p}_1^0-\epsilon_b+i0)}\\
\times\left[\sum_{\epsilon_n\neq\epsilon_a}\frac{\langle PaPb|I(\mathrm{p}_1'^0-\mathrm{p}_1^0)|nb\rangle\langle n|\Sigma(\mathrm{p}_1^0)|a\rangle}{\mathrm{p}_1^0-\epsilon_n(1-i0)}+\sum_{\epsilon_n\neq\epsilon_b}\frac{\langle PaPb|I(\mathrm{p}_1'^0-\mathrm{p}_1^0)|an\rangle\langle n|\Sigma(E-\mathrm{p}_1^0)|b\rangle}{E-\mathrm{p}_1^0-\epsilon_n(1-i0)}\right.\\
\left.+\sum_{\epsilon_n\neq\epsilon_{Pa}}\frac{\langle Pa|\Sigma(\mathrm{p}_1'^0)|n\rangle\langle nPb|I(\mathrm{p}_1'^0-\mathrm{p}_1^0)|ab\rangle}{\mathrm{p}_1'^0-\epsilon_n(1-i0)}+\sum_{\epsilon_n\neq\epsilon_{Pb}}\frac{\langle Pb|\Sigma(E-\mathrm{p}_1'^0)|n\rangle\langle Pan|I(\mathrm{p}_1'^0-\mathrm{p}_1^0)|ab\rangle}{E-\mathrm{p}_1'^0-\epsilon_n(1-i0)}\right].\end{aligned} \tag{15}$$

Using the identity

$$\frac{1}{(\mathrm{p}^0-\epsilon_a+i0)(E-\mathrm{p}^0-\epsilon_b+i0)}=\frac{1}{\Delta E}\left(\frac{1}{\mathrm{p}^0-\epsilon_a+i0}+\frac{1}{E-\mathrm{p}^0-\epsilon_b+i0}\right), \tag{16}$$

we obtain

$$\Delta E_{\rm ir}=\frac{1}{2\pi i}\oint_\Gamma dE\,\frac{1}{\Delta E}\left\{\left(\frac{i}{2\pi}\right)^2\sum_P(-1)^P\int_{-\infty}^{\infty}d{\rm p}_1^0\,d{\rm p}_1'^0\left(\frac{1}{{\rm p}_1'^0-\epsilon_{Pa}+i0}+\frac{1}{E-{\rm p}_1'^0-\epsilon_{Pb}+i0}\right)\right.$$
$$\times\left(\frac{1}{{\rm p}_1^0-\epsilon_a+i0}+\frac{1}{E-{\rm p}_1^0-\epsilon_b+i0}\right)\left[\sum_{\epsilon_n\neq\epsilon_a}\frac{\langle PaPb|I({\rm p}_1'^0-{\rm p}_1^0)|nb\rangle\langle n|\Sigma({\rm p}_1^0)|a\rangle}{{\rm p}_1^0-\epsilon_n(1-i0)}\right.$$
$$+\sum_{\epsilon_n\neq\epsilon_b}\frac{\langle PaPb|I({\rm p}_1'^0-{\rm p}_1^0)|an\rangle\langle n|\Sigma(E-{\rm p}_1^0)|b\rangle}{E-{\rm p}_1^0-\epsilon_n(1-i0)}+\sum_{\epsilon_n\neq\epsilon_{Pa}}\frac{\langle Pa|\Sigma({\rm p}_1'^0)|n\rangle\langle nPb|I({\rm p}_1'^0-{\rm p}_1^0)|ab\rangle}{{\rm p}_1'^0-\epsilon_n(1-i0)}$$
$$\left.\left.+\sum_{\epsilon_n\neq\epsilon_{Pb}}\frac{\langle Pb|\Sigma(E-{\rm p}_1'^0)|n\rangle\langle Pan|I({\rm p}_1'^0-{\rm p}_1^0)|ab\rangle}{E-{\rm p}_1'^0-\epsilon_n(1-i0)}\right]\right\}. \tag{17}$$

The expression in the curly braces is analytical in E inside of Γ, if the photon mass is chosen to keep all the cuts outside this contour (see Refs. [16,17] for details). Calculating the first-order residual at $E=E_n^{(0)}$ and using the identity

$$\frac{i}{2\pi}\left(\frac{1}{x+i0}+\frac{1}{-x+i0}\right)=\delta(x), \tag{18}$$

we obtain the final expression for the irreducible contribution

$$\Delta E_{\rm ir}=\sum_P(-1)^P$$
$$\times\left\{\sum_{\epsilon_n\neq\epsilon_a}\langle PaPb|I(\Delta)|nb\rangle\frac{1}{\epsilon_a-\epsilon_n}\langle n|\Sigma(\epsilon_a)|a\rangle\right.$$
$$+\sum_{\epsilon_n\neq\epsilon_b}\langle PaPb|I(\Delta)|an\rangle\frac{1}{\epsilon_b-\epsilon_n}\langle n|\Sigma(\epsilon_b)|b\rangle$$
$$+\sum_{\epsilon_n\neq\epsilon_{Pa}}\langle Pa|\Sigma(\epsilon_{Pa})|n\rangle\frac{1}{\epsilon_{Pa}-\epsilon_n}\langle nPb|I(\Delta)|ab\rangle$$
$$\left.+\sum_{\epsilon_n\neq\epsilon_{Pb}}\langle Pb|\Sigma(\epsilon_{Pb})|n\rangle\frac{1}{\epsilon_{Pb}-\epsilon_n}\langle Pan|I(\Delta)|ab\rangle\right\}, \tag{19}$$

where $\Delta=\epsilon_{Pa}-\epsilon_a$. For the numerical evaluation it is more convenient to write Eq. (19) as a sum of nondiagonal matrix elements of the self-energy operator,

$$\Delta E_{\rm ir}=2\{\langle a|\Sigma(\epsilon_a)|\xi_a\rangle+\langle b|\Sigma(\epsilon_b)|\xi_b\rangle\}, \tag{20}$$

where

$$|\xi_a\rangle=\sum_{\epsilon_n\neq\epsilon_a}\frac{|n\rangle}{\epsilon_a-\epsilon_n}\sum_P(-1)^P\langle PaPb|I(\Delta)|nb\rangle, \tag{21}$$

$$|\xi_b\rangle=\sum_{\epsilon_n\neq\epsilon_b}\frac{|n\rangle}{\epsilon_b-\epsilon_n}\sum_P(-1)^P\langle PaPb|I(\Delta)|an\rangle. \tag{22}$$

B. Vertex contribution

The Feynman rules yield for the vertex contribution,

$$\Delta E_{\rm ver}=\frac{1}{2\pi i}\oint_\Gamma dE\,\Delta E\left(\frac{i}{2\pi}\right)^3\sum_P(-1)^P\sum_{n_1n_2}\int_{-\infty}^{\infty}d{\rm p}_1^0\,d{\rm p}_1'^0$$
$$\times\frac{1}{({\rm p}_1'^0-\epsilon_{Pa}+i0)(E-{\rm p}_1'^0-\epsilon_{Pb}+i0)}\,\frac{1}{({\rm p}_1^0-\epsilon_a+i0)(E-{\rm p}_1^0-\epsilon_b+i0)}$$
$$\times\int_{-\infty}^{\infty}d\omega\left[\frac{\langle n_1Pb|I({\rm p}_1'^0-{\rm p}_1^0)|n_2b\rangle\langle Pan_2|I(\omega)|n_1a\rangle}{[{\rm p}_1'^0-\omega-\epsilon_{n_1}(1-i0)][{\rm p}_1^0-\omega-\epsilon_{n_2}(1-i0)]}\right.$$
$$\left.+\frac{\langle Pan_1|I({\rm p}_1'^0-{\rm p}_1^0)|an_2\rangle\langle Pbn_2|I(\omega)|n_1b\rangle}{[E-{\rm p}_1'^0-\omega-\epsilon_{n_1}(1-i0)][E-{\rm p}_1^0-\omega-\epsilon_{n_2}(1-i0)]}\right]. \tag{23}$$

Calculating the integrals over E, ${\rm p}_1^0$, and ${\rm p}_1'^0$ in the same way as for the irreducible contribution, we obtain

$$\Delta E_{\rm ver}=\sum_P\,(-1)^P\sum_{n_1n_2}\frac{i}{2\pi}\int_{-\infty}^{\infty}d\omega\left[\frac{\langle n_1Pb|I(\Delta)|n_2b\rangle\langle Pan_2|I(\omega)|n_1a\rangle}{[\epsilon_{Pa}-\omega-\epsilon_{n_1}(1-i0)][\epsilon_a-\omega-\epsilon_{n_2}(1-i0)]}\right.$$
$$\left.+\frac{\langle Pan_1|I(\Delta)|an_2\rangle\langle Pbn_2|I(\omega)|n_1b\rangle}{[\epsilon_{Pb}-\omega-\epsilon_{n_1}(1-i0)][\epsilon_b-\omega-\epsilon_{n_2}(1-i0)]}\right]. \tag{24}$$

C. Reducible contribution

As mentioned earlier, the reducible part of the diagrams in Fig. 1(a) is calculated together with the second term in Eq. (6):

$$\Delta E_{\rm red}=\Delta\tilde{E}_{\rm red}-\frac{1}{2\pi i}\oint_\Gamma dE\,\Delta E\,\Delta g^{(1)}_{nn}(E)\frac{1}{2\pi i}\oint_\Gamma dE'\Delta g^{(1)}_{nn}(E'). \tag{25}$$

The $\Delta\tilde{E}_{\rm red}$ contribution is defined by Fig. 3. The Feynman rules yield

$$\Delta\tilde{E}_{\rm red}=\frac{1}{2\pi i}\oint_\Gamma dE\,\Delta E\left(\frac{i}{2\pi}\right)^2\sum_P\,(-1)^P\int_{-\infty}^{\infty}d{\rm p}_1^0\,d{\rm p}_1'^0\frac{\langle PaPb|I({\rm p}_1'^0-{\rm p}_1^0)|ab\rangle}{({\rm p}_1'^0-\epsilon_{Pa}+i0)(E-{\rm p}_1'^0-\epsilon_{Pb}+i0)({\rm p}_1^0-\epsilon_a+i0)(E-{\rm p}_1^0-\epsilon_b+i0)}$$
$$\times\left[\frac{\langle a|\Sigma({\rm p}_1^0)|a\rangle}{{\rm p}_1^0-\epsilon_a+i0}+\frac{\langle b|\Sigma(E-{\rm p}_1^0)|b\rangle}{E-{\rm p}_1^0-\epsilon_b+i0}+\frac{\langle Pa|\Sigma({\rm p}_1'^0)|Pa\rangle}{{\rm p}_1'^0-\epsilon_{Pa}+i0}+\frac{\langle Pb|\Sigma(E-{\rm p}_1'^0)|Pb\rangle}{E-{\rm p}_1'^0-\epsilon_{Pb}+i0}\right]. \tag{26}$$

For brevity, we demonstrate the integration over E, ${\rm p}_1^0$, and ${\rm p}_1'^0$ only for the first term in the square brackets (we refer to it as $\Delta\tilde{E}^{(1)}_{\rm red}$). Using Eq. (16) and the identity

$$\frac{1}{({\rm p}^0-\epsilon_a+i0)^2(E-{\rm p}^0-\epsilon_b+i0)}=\frac{1}{(\Delta E)^2}\left(\frac{1}{{\rm p}^0-\epsilon_a+i0}+\frac{1}{E-{\rm p}^0-\epsilon_b+i0}\right)+\frac{1}{\Delta E}\frac{1}{({\rm p}^0-\epsilon_a+i0)^2}, \tag{27}$$

we write the expression for $\Delta\tilde{E}^{(1)}_{\rm red}$ as

$$\Delta\tilde{E}^1_{\rm red}=\frac{1}{2\pi i}\oint_\Gamma dE\left(\frac{i}{2\pi}\right)^2\sum_P\,(-1)^P\int_{-\infty}^{\infty}d{\rm p}_1^0\,d{\rm p}_1'^0\langle PaPb|I({\rm p}_1'^0-{\rm p}_1^0)|ab\rangle\langle a|\Sigma({\rm p}_1^0)|a\rangle$$
$$\times\left\{\frac{1}{\Delta E}\left(\frac{1}{{\rm p}_1'^0-\epsilon_{Pa}+i0}+\frac{1}{E-{\rm p}_1'^0-\epsilon_{Pb}+i0}\right)\frac{1}{({\rm p}_1^0-\epsilon_a+i0)^2}\right.$$
$$\left.+\frac{1}{(\Delta E)^2}\left(\frac{1}{{\rm p}_1'^0-\epsilon_{Pa}+i0}+\frac{1}{E-{\rm p}_1'^0-\epsilon_{Pb}+i0}\right)\left(\frac{1}{{\rm p}_1^0-\epsilon_a+i0}+\frac{1}{E-{\rm p}_1^0-\epsilon_b+i0}\right)\right\}. \tag{28}$$

Integrating over E and utilizing Eq. (18), we obtain

$$\Delta\tilde{E}^1_{\rm red}=\sum_P\,(-1)^P\frac{i}{2\pi}\left\{-\int_{-\infty}^{\infty}d{\rm p}_1'^0\frac{\langle PaPb|I({\rm p}_1'^0-\epsilon_a)|ab\rangle\langle a|\Sigma(\epsilon_a)|a\rangle}{(\epsilon_{Pa}-{\rm p}_1'^0+i0)^2}\right.$$
$$\left.+\int_{-\infty}^{\infty}d{\rm p}_1^0\langle PaPb|I(\epsilon_{Pa}-{\rm p}_1^0)|ab\rangle\langle a|\Sigma({\rm p}_1^0)|a\rangle\left[\frac{1}{({\rm p}_1^0-\epsilon_a+i0)^2}-\frac{1}{({\rm p}_1^0-\epsilon_a-i0)^2}\right]\right\}. \tag{29}$$

Taking into account that

$$\frac{1}{(x+i0)^2}-\frac{1}{(x-i0)^2}=-\frac{2\pi}{i}\frac{d}{dx}\delta(x) \tag{30}$$

and integrating by parts, we obtain

$$\Delta\tilde{E}^{(1)}_{\rm red}=\sum_P(-1)^P\Bigg\{-\frac{i}{2\pi}\int_{-\infty}^{\infty}d{\rm p}_1'^0 \times\frac{\langle PaPb|I({\rm p}_1'^0-\epsilon_a)|ab\rangle\langle a|\Sigma(\epsilon_a)|a\rangle}{(\epsilon_{Pa}-{\rm p}_1'^0+i0)^2} +\langle PaPb|I(\Delta)|ab\rangle\langle a|\Sigma'(\epsilon_a)|a\rangle -\langle PaPb|I'(\Delta)|ab\rangle\langle a|\Sigma(\epsilon_a)|a\rangle\Bigg\}, \tag{31}$$

where $\Sigma'(\epsilon_a)=d\Sigma(\epsilon)/d\epsilon|_{\epsilon=\epsilon_a}$ and $I'(\Delta)=dI(\omega)/d\omega|_{\omega=\Delta}$. The contributions of the other terms in the square brackets of Eq. (26) can be evaluated in the same way:

$$\Delta\tilde{E}^{(2)}_{\rm red}=\sum_P(-1)^P\Bigg\{-\frac{i}{2\pi}\int_{-\infty}^{\infty}d{\rm p}_1'^0 \times\frac{\langle PaPb|I({\rm p}_1'^0-\epsilon_a)|ab\rangle\langle b|\Sigma(\epsilon_b)|b\rangle}{(\epsilon_{Pa}-{\rm p}_1'^0+i0)^2} +\langle PaPb|I(\Delta)|ab\rangle\langle b|\Sigma'(\epsilon_b)|b\rangle\Bigg\}, \tag{32}$$

$$\Delta\tilde{E}^{(3)}_{\rm red}=\sum_P(-1)^P\Bigg\{-\frac{i}{2\pi}\int_{-\infty}^{\infty}d{\rm p}_1^0 \times\frac{\langle PaPb|I(\epsilon_{Pa}-{\rm p}_1^0)|ab\rangle\langle Pa|\Sigma(\epsilon_{Pa})|Pa\rangle}{(\epsilon_a-{\rm p}_1^0+i0)^2} +\langle PaPb|I(\Delta)|ab\rangle\langle Pa|\Sigma'(\epsilon_{Pa})|Pa\rangle +\langle PaPb|I'(\Delta)|ab\rangle\langle Pa|\Sigma(\epsilon_{Pa})|Pa\rangle\Bigg\}, \tag{33}$$

$$\Delta\tilde{E}^{(4)}_{\rm red}=\sum_P(-1)^P\Bigg\{-\frac{i}{2\pi}\int_{-\infty}^{\infty}d{\rm p}_1^0 \times\frac{\langle PaPb|I(\epsilon_{Pa}-{\rm p}_1^0)|ab\rangle\langle Pb|\Sigma(\epsilon_{Pb})|Pb\rangle}{(\epsilon_a-{\rm p}_1^0+i0)^2} +\langle PaPb|I(\Delta)|ab\rangle\langle Pb|\Sigma'(\epsilon_{Pb})|Pb\rangle\Bigg\}. \tag{34}$$

Using Eq. (30), we obtain for the sum of Eqs. (31)–(34),

$$\Delta\tilde{E}_{\rm red}=\sum_P(-1)^P\Bigg\{2\langle PaPb|I(\Delta)|ab\rangle[\langle a|\Sigma'(\epsilon_a)|a\rangle +\langle b|\Sigma'(\epsilon_b)|b\rangle]-\frac{i}{2\pi}\int_{-\infty}^{\infty}dw\langle PaPb|I(\omega)|ab\rangle \times\left(\frac{1}{(\omega-\Delta-i0)^2}+\frac{1}{(\omega+\Delta-i0)^2}\right) \times[\langle a|\Sigma(\epsilon_a)|a\rangle+\langle b|\Sigma(\epsilon_b)|b\rangle]\Bigg\} +\langle ba|I'(\Delta)|ab\rangle[\langle a|\Sigma(\epsilon_a)|a\rangle-\langle b|\Sigma(\epsilon_b)|b\rangle]. \tag{35}$$

Let us consider the evaluation of the second term in Eq. (25). We denote the contributions to $\Delta g^{(1)}_{nn}$ from the diagrams in Figs. 2(a) and 2(b) by $\Delta g^{(1)}_{\rm 1ph}$ and $\Delta g^{(1)}_{SE}$, respectively. A simple calculation yields

$$\frac{1}{2\pi i}\oint_\Gamma dE\,\Delta E\,\Delta g^{(1)}_{\rm 1ph}=\sum_P(-1)^P\langle PaPb|I(\Delta)|ab\rangle, \tag{36}$$

$$\frac{1}{2\pi i}\oint_\Gamma dE\,\Delta E\Delta g^{(1)}_{SE}=\langle a|\Sigma(\epsilon_a)|a\rangle+\langle b|\Sigma(\epsilon_b)|b\rangle, \tag{37}$$

$$\frac{1}{2\pi i}\oint_\Gamma dE\,\Delta g^{(1)}_{\rm 1ph}=\sum_P(-1)^P\frac{i}{2\pi}\int_{-\infty}^{\infty}dw\langle PaPb|I(\omega)|ab\rangle \times\left(\frac{1}{(\omega-\Delta-i0)^2}+\frac{1}{(\omega+\Delta-i0)^2}\right), \tag{38}$$

$$\frac{1}{2\pi i}\oint_\Gamma dE\,\Delta g^{(1)}_{SE}=\langle a|\Sigma'(\epsilon_a)|a\rangle+\langle b|\Sigma'(\epsilon_b)|b\rangle. \tag{39}$$

Combining Eq. (35) and Eqs. (36)–(39), we obtain the final expression for the reducible contribution. For further evaluation it is convenient to separate this contribution into two parts,

$$\Delta E_{\rm red}=\Delta E^A_{\rm red}+\Delta E^B_{\rm red}, \tag{40}$$

$$\Delta E^A_{\rm red}=\langle ba|I'(\Delta)|ab\rangle[\langle a|\Sigma(\epsilon_a)|a\rangle-\langle b|\Sigma(\epsilon_b)|b\rangle], \tag{41}$$

$$\Delta E^B_{\rm red}=\Delta E_{\rm 1ph}[\langle a|\Sigma'(\epsilon_a)|a\rangle+\langle b|\Sigma'(\epsilon_b)|b\rangle], \tag{42}$$

where $\Delta E_{\rm 1ph}=\Sigma_P(-1)^P\langle PaPb|I(\Delta)|ab\rangle$ is the one-photon exchange correction.

D. Removing divergences

The formulas presented so far are only formal expressions and require renormalization. According to Eq. (20), the irreducible contribution can be written as a sum of nondiagonal matrix elements of the self-energy operator. Thus, the renormalization scheme developed for the first-order self-energy correction can be used in this case. Our procedure for the evaluation of the first-order self-energy is described in Ref.

[14]. Only a slight generalization of those formulas for the case of a nondiagonal matrix element is needed.

The $\Delta E^A_{\rm red}$ correction consists of two first-order self-energy corrections multiplied by a simple factor. Its calculation causes no problems and was performed in the same way.

Let us consider the renormalization of the $\Delta E_{\rm ver}$ and the $\Delta E^B_{\rm red}$ term. To cancel ultraviolet divergences explicitly, we separate contributions of the free-electron propagators (we refer to them as *free* terms and to the remainder as *many-potential* terms):

$$\Delta E_{\rm ver}+\Delta E^B_{\rm red}=\Delta E^{(0)}_{\rm vr}+\Delta E^{\rm many}_{\rm vr}, \tag{43}$$

where

$$\Delta E^{(0)}_{\rm vr}=\Delta E^{(0)}_{\rm ver}+\Delta E^{B(0)}_{\rm red}, \tag{44}$$

$$\Delta E^{\rm many}_{\rm vr}=\Delta E^{\rm many}_{\rm ver}+\Delta E^{B,\rm many}_{\rm red}. \tag{45}$$

Only the free contributions contain ultraviolet divergences. To separate divergent terms explicitly, we evaluate these contributions in momentum space using dimensional regularization. We will show below that

$$\Delta E^{(0)}_{\rm ver}=\Delta E_{1\rm ph}\frac{\alpha}{2\pi}\Delta_\epsilon+\Delta E^{(0)}_{{\rm ver},R}, \tag{46}$$

$$\Delta E^{B(0)}_{\rm red}=-\Delta E_{1\rm ph}\frac{\alpha}{2\pi}\Delta_\epsilon+\Delta E^{B(0)}_{{\rm red},R}, \tag{47}$$

where Δ_ϵ is the ultraviolet divergent constant, $\Delta E_{1\rm ph}$ is the one-photon exchange correction, and contributions with the subscript ''R'' are free from ultraviolet divergences. The ultraviolet divergent terms cancel each other in the sum. Thus, Eq. (44) can be replaced by

$$\Delta E^{(0)}_{\rm vr}=\Delta E^{(0)}_{{\rm ver},R}+\Delta E^{B(0)}_{{\rm red},R}. \tag{48}$$

As a result, we have for the δE^b_a correction (11),

$$\delta E^b_a=\Delta E^{(0)}_{\rm vr}+\Delta E^{\rm many}_{\rm vr}+\Delta E_{\rm ir}+\Delta E^A_{\rm red}. \tag{49}$$

Note that the $\Delta E^A_{\rm red}$ contribution vanishes for the δE^{1s}_{1s} correction.

We note that both $\Delta E^{\rm many}_{\rm ver}$ and $\Delta E^{B,\rm many}_{\rm red}$ are infrared divergent. The singularities cancel each other in the sum and the $\Delta E^{\rm many}_{\rm vr}$ correction is free from any divergences. However, for the numerical evaluation one should separate and cancel infrared divergences explicitly. A nonintegrable singularity arises in vertex contribution (24) when both poles appear at $\omega=0$ simultaneously. The expression for reducible contribution (42) contains the derivative of the self-energy operator with respect to the energy. It yields a squared energy denominator, which causes an infrared singularity when the pole appears at $\omega=0$. The divergent terms can be easily separated and calculated together to obtain a finite result.

II. ANGULAR INTEGRATIONS

In the previous section we obtained general formulas for the two-electron self-energy correction δE^b_a representing the interaction of electrons in the states a and b. Let us consider now the corrections representing the interaction of the valence electron with the closed-shell core, namely, $\delta E^{(1s)}_{2s}$ and $\delta E^{(1s)}_{2p}$ corrections. To obtain expressions for these corrections, the summation over magnetic quantum numbers of core electrons should be carried out in the formulas presented so far. In this section our technique of angular integration is described and expressions in a form suitable for numerical evaluation are obtained. We denote valence and core electrons with indices ''v'' and ''c,'' respectively.

As indicated in the previous section, the $\delta E^{(c)}_v$ correction can be expressed as a sum of four components,

$$\Delta E^{(c)}_v=\Delta E^{(0)}_{\rm vr}+\Delta E^{\rm many}_{\rm vr}+\Delta E_{\rm ir}+\Delta E^A_{\rm red}. \tag{50}$$

In the following we consider each of these components separately.

A. $\Delta E^{(0)}_{\rm vr}$ correction

The $\Delta E^{(0)}_{\rm vr}$ correction is given by the sum of the free contributions of the vertex and the reducible term, as it is stated by Eq. (44). The free reducible term is the contribution of the free-electron propagators in Eq. (42). After transformation into momentum space, we have

$$\begin{aligned}\Delta E^{B(0)}_{\rm red}=&\sum_{\mu_c}\left[\sum_P(-1)^P\langle PcPv|I(\Delta)|cv\rangle\right]\\&\times\int\frac{d\mathbf{p}}{(2\pi)^3}\left\{\overline{\psi}_c(\mathbf{p})\left.\frac{\partial\Sigma^{(0)}(\mathrm{p})}{\partial \mathrm{p}^0}\right|_{\mathbf{p}^0=\epsilon_c}\psi_c(\mathbf{p})\right.\\&\left.+\overline{\psi}_v(\mathbf{p})\left.\frac{\partial\Sigma^{(0)}(\mathrm{p})}{\partial \mathrm{p}^0}\right|_{\mathbf{p}^0=\epsilon_v}\psi_v(\mathbf{p})\right\},\end{aligned} \tag{51}$$

where μ_c is the magnetic quantum number of the core electron and $\Sigma^{(0)}(\mathrm{p})$ denotes the free self-energy operator. Its derivative with respect to the energy reads

$$\frac{\partial\Sigma^{(0)}(\mathbf{p})}{\partial\epsilon}=-\frac{\alpha}{4\pi}\left\{\gamma_0\Delta_\epsilon+\frac{\not{\mathrm{p}}}{m^2}a_1(\rho)+\gamma_0 a_2(\rho)+a_3(\rho)\right\}, \tag{52}$$

$$a_1(\rho)=-\frac{2\epsilon}{(1-\rho)^2}\left(3-\rho+\frac{2}{1-\rho}\ln\rho\right), \tag{53}$$

$$a_2(\rho)=2+\frac{\rho}{1-\rho}\left(1+\frac{2-\rho}{1-\rho}\ln\rho\right), \tag{54}$$

$$a_3(\rho)=\frac{8\epsilon}{m(1-\rho)}\left(1+\frac{1}{1-\rho}\ln\rho\right), \tag{55}$$

where $\mathrm{p}=(\epsilon,\mathbf{p})$ and $\rho=1-\mathrm{p}^2/m^2$. For details we refer to [14]. Integration over the angular variables yields

$$\begin{aligned}\Delta E^{B(0)}_{\rm red}=-\frac{\alpha}{4\pi}\Delta E_{1\rm ph}\Bigg(&2\Delta_\epsilon+\sum_{n=c,v}\int_0^\infty\frac{p^2\,dp}{(2\pi)^3}\{a_1(\rho_n)\\&\times[\epsilon_n(\tilde{g}_n^2+\tilde{f}_n^2)+2p\tilde{f}_n\tilde{g}_n]+a_2(\rho_n)(\tilde{g}_n^2+\tilde{f}_n^2)\\&+a_3(\rho_n)(\tilde{g}_n^2-\tilde{f}_n^2)\}\Bigg).\end{aligned} \tag{56}$$

Here $\Delta E_{1\mathrm{ph}}=\Sigma_{\mu_c}[\Sigma_P(-1)^P\langle PcPv|I(\Delta)|cv\rangle]$ is the correction due to the one-photon exchange of the valence electron with the closed-shell core, $p=|\mathbf{p}|$, and $\tilde{g}_n=\tilde{g}_n(p)$ and $\tilde{f}_n=\tilde{f}_n(p)$ are the components of the momentum-space wave function. We use the Dirac wave functions written in the form

$$\psi_a(\mathbf{x})=\begin{pmatrix} g_a(x)\chi_{\kappa_a m_a}(\hat{\mathbf{x}}) \\ if_a(x)\chi_{-\kappa_a m_a}(\hat{\mathbf{x}}) \end{pmatrix}, \tag{57}$$

where $\chi_{\kappa\mu}(\hat{\mathbf{x}})$ is the spin-angular spinor [18]. The momentum-space wave functions are defined by

$$\psi_a(\mathbf{p})=\int d\mathbf{x}e^{-i\mathbf{px}}\psi_a(\mathbf{x})=i^{-l_a}\begin{pmatrix} \tilde{g}_a(p)\chi_{\kappa_a m_a}(\hat{\mathbf{p}}) \\ \tilde{f}_a(p)\chi_{-\kappa_a m_a}(\hat{\mathbf{p}}) \end{pmatrix}. \tag{58}$$

Here κ denotes the Dirac angular-momentum quantum number, $l=|\kappa+\frac{1}{2}|-\frac{1}{2}$.

The free vertex correction $\Delta E^{(0)}_{\mathrm{ver}}$ can be obtained from expression (24) for ΔE_{ver} by substituting the free Dirac states for the bound-state solutions. As is well known, for a separation of ultraviolet divergences, it is more convenient to work in momentum space. For further evaluation we transform the expression for the free-vertex contribution partly into the momentum-space representation:

$$\begin{aligned}\Delta E^{(0)}_{\mathrm{ver}}=\alpha\sum_P\frac{(-1)^P}{2j_v+1}\sum_{\mu_c\mu_v}\int\frac{d\mathbf{p}}{(2\pi)^3}\int\frac{d\mathbf{p}'}{(2\pi)^3}\\ \times\{\overline{\psi}_{Pc}(\mathbf{p})A^{Pvv}_\mu(\mathbf{q})\Gamma^\mu(\mathrm{p},\mathrm{p}')\big|_{\substack{\mathbf{p}'^0=\epsilon_c\\ \mathbf{p}^0=\epsilon_{Pc}}}\psi_c(\mathbf{p}')\\ +\overline{\psi}_{Pv}(\mathbf{p})A^{Pcc}_\mu(\mathbf{q})\Gamma^\mu(\mathrm{p},\mathrm{p}')\big|_{\substack{\mathbf{p}'^0=\epsilon_v\\ \mathbf{p}^0=\epsilon_{Pv}}}\psi_v(\mathbf{p}')\},\end{aligned} \tag{59}$$

where

$$A^{ab}_\mu(\mathbf{q})=\frac{4\pi}{\mathbf{q}^2-\Delta^2_{ab}-i0}\int d\mathbf{z}\,\psi^\dagger_a(\mathbf{z})\alpha_\mu\psi_b(\mathbf{z})e^{-i\mathbf{qz}}. \tag{60}$$

Here $\Gamma^\mu(\mathrm{p},\mathrm{p}')$ is the free-vertex operator defined in Appendix A, $\Delta_{ab}=\epsilon_a-\epsilon_b$, $\mathbf{q}=\mathbf{p}-\mathbf{p}'$, and $\psi_n(\mathbf{p})$ and $\psi_n(\mathbf{z})$ are the wave functions in momentum-space and coordinate-space representation, respectively. Note, that in Eq. (59) we average over magnetic substates of the valence electron.

The free-vertex operator in Eq. (59) contains ultraviolet divergence, which can be separated explicitly (see Appendix A):

$$\Gamma^\mu(\mathrm{p},\mathrm{p}')=\frac{\alpha}{4\pi}\Delta_\epsilon\gamma^\mu+\Gamma^\mu_R(\mathrm{p},\mathrm{p}'). \tag{61}$$

According to this, we write the free vertex correction as

$$\Delta E^{(0)}_{\mathrm{ver}}=\Delta E_{1\mathrm{ph}}\frac{\alpha}{2\pi}\Delta_\epsilon+\Delta E^{(0)}_{\mathrm{ver},R}. \tag{62}$$

The second term of this expression is finite and the first term has a simple structure. Obviously, the ultraviolet divergent term in Eq. (62) is cancelled by the corresponding term from free reducible contribution (56).

Let us consider the evaluation of the integrals over angular variables in $\Delta E^{(0)}_{\mathrm{ver},R}$. It is convenient to divide this correction into two contributions: *direct* part ($Pc,Pv=c,v$) and *exchange* part ($Pc,Pv=v,c$):

$$\Delta E^{(0)}_{\mathrm{ver},R}=\Delta E^{(0),\mathrm{dir}}_{\mathrm{ver}}+\Delta E^{(0),\mathrm{exch}}_{\mathrm{ver}}. \tag{63}$$

1. Direct part of the free vertex contribution

The evaluation of the $\Delta E^{(0),\mathrm{dir}}_{\mathrm{ver}}$ correction is relatively easy. Angular integration for $A_\mu=(A_0,\mathbf{A})$ leads to

$$\sum_{\mu_a}A^{aa}_0(\mathbf{q})=\frac{8\pi}{q^2}R^{1,aa}_0(q), \tag{64}$$

$$\sum_{\mu_a}\mathbf{A}^{aa}(\mathbf{q})=0, \tag{65}$$

where $q=|\mathbf{q}|$ and the radial integrals $R^{1,ab}_L(q)$ are determined by

$$R^{1,ab}_L(q)=\int_0^\infty dz\,z^2j_L(qz)\{g_a(z)g_b(z)+f_a(z)f_b(z)\}. \tag{66}$$

$j_L(z)$ denotes the spherical Bessel function. Taking into account Eq. (A3), we obtain

$$\begin{aligned}\Delta E^{(0),\mathrm{dir}}_{\mathrm{ver}}=\frac{\alpha^2}{16\pi^5}\int_0^\infty dp\int_0^\infty dp'\int_{-1}^1 d\xi\frac{p^2p'^2}{q^2}\\ \times\{R^{1,vv}_0(q)[\mathcal{F}^{cc}_1P_{l_c}(\xi)+\mathcal{F}^{cc}_2P_{\bar{l}_c}(\xi)]\\ +R^{1,cc}_0(q)[\mathcal{F}^{vv}_1P_{l_v}(\xi)+\mathcal{F}^{vv}_2P_{\bar{l}_v}(\xi)]\},\end{aligned} \tag{67}$$

where $p=|\mathbf{p}|$, $p'=|\mathbf{p}'|$, $\xi=\hat{\mathbf{p}}\cdot\hat{\mathbf{p}}'$, and $P_l(\xi)$ is a Legendre polynomial, $\bar{l}=2j-l$.

2. Exchange part of the free-vertex contribution

Let us consider the evaluation of $\Delta E^{(0),\mathrm{exch}}_{\mathrm{ver}}$. Using the symmetry condition $\Gamma^\mu(\mathrm{p},\mathrm{p}')=\Gamma^\mu(\mathrm{p}',\mathrm{p})$, one can show that both terms in the expression for the $\Delta E^{(0),\mathrm{exch}}_{\mathrm{ver}}$ correction provide the same contribution. Thus, we can write

$$\begin{aligned}\Delta E^{(0),\mathrm{exch}}_{\mathrm{ver}}=-\frac{2\alpha}{2j_v+1}\sum_{\mu_c\mu_v}\int\frac{d\mathbf{p}}{(2\pi)^3}\int\frac{d\mathbf{p}'}{(2\pi)^3}\\ \times\overline{\psi}_v(\mathbf{p})\Gamma^\mu_R(\mathrm{p},\mathrm{p}')\big|_{\substack{\mathbf{p}'^0=\epsilon_c\\ \mathbf{p}^0=\epsilon_v}}\psi_c(\mathbf{p}')A^{cv}_\mu(\mathbf{q}).\end{aligned} \tag{68}$$

Angular integration for $A_\mu=(A_0,\mathbf{A})$ yields

$$\begin{aligned}A^{ab}_0(\mathbf{q})=\frac{16\pi^2}{\mathbf{q}^2-\Delta^2_{ab}-i0}\\ \times\sum_{LM}i^{-L}s^{ba}_{LM}Y_{LM}(\hat{\mathbf{q}})C_L(\kappa_b,\kappa_a)R^{1,ab}_L(q),\end{aligned} \tag{69}$$

$$\mathbf{A}^{ab}(\mathbf{q})=\frac{16\pi^2}{\mathbf{q}^2-\Delta_{ab}^2-i0}\times\sum_{JLM} i^{1-L}s_{JM}^{ba}\mathbf{Y}_{JLM}(\hat{\mathbf{q}})R_{JL}^{2,ab}(q), \tag{70}$$

where $Y_{LM}(\hat{\mathbf{q}})$ denotes a spherical harmonic, $\mathbf{Y}_{JLM}(\hat{\mathbf{q}})$ is the vector spherical harmonic defined by Eq. (B5), the coefficients s_{JM}^{ab} are defined by Eq. (B2), and the coefficients $C_L(\kappa_1,\kappa_2)$ are given by Eq. (C10). The radial integrals $R_{JL}^{2,ab}$ are determined by

$$R_{JL}^{2,ab}(q)=\int_0^\infty dz\, z^2 j_L(qz)\{g_a(z)f_b(z)S_{JL}(\kappa_a,-\kappa_b)-f_a(z)g_b(z)S_{JL}(-\kappa_a,\kappa_b)\}, \tag{71}$$

where the coefficients $S_{JL}(\kappa_1,\kappa_2)$ are defined by Eqs. (C7)–(C9).

For further evaluation of $\Delta E_{\rm ver}^{(0),\rm exch}$, we substitute Eqs. (A3), (A4), (69), and (70) into Eq. (68) and integrate over the angular variables. In this case the angular integration is much more tedious than for the direct part. For brevity, we demonstrate the angular integration for the special case $c=1s$, $v=2p_{1/2}$ and only for the part of $\Delta E_{\rm ver}^{(0),\rm exch}$ that results from the third term in Eq. (A4). This example shows all the essential features of the evaluation of the other terms. We refer to this part as ΔE_{34}:

$$\Delta E_{34}=i\frac{\alpha^2}{4\pi}\sum_{\mu_{2p}\mu_{1s}}\int\frac{d\mathbf{p}}{(2\pi)^3}\int\frac{d\mathbf{p}'}{(2\pi)^3}\times(\mathcal{R}_3^{2p1s}\mathbf{p}+\mathcal{R}_4^{2p1s}\mathbf{p}')\times\chi_{1\mu_{2p}}^\dagger(\hat{\mathbf{p}})\chi_{-1\mu_{1s}}(\hat{\mathbf{p}}')\mathbf{A}^{1s2p}(\mathbf{q}). \tag{72}$$

In this case expression (70) is reduced to

$$\mathbf{A}^{1s2p}(\mathbf{q})=\frac{16\pi^2}{\mathbf{q}^2-\Delta_{2p1s}^2-i0}\times\sum_{L=0,2}\sum_M i^{1-L}s_{1M}^{2p1s}\mathbf{Y}_{1LM}(\hat{\mathbf{q}})R_{1L}^{2,1s2p}(q). \tag{73}$$

To perform the angular integration, we have to evaluate an expression

$$J\equiv\sum_{\mu_{1s}\mu_{2p}M} s_{1M}^{2p1s}(\hat{\mathbf{p}}\cdot\mathbf{Y}_{1LM}(\hat{\mathbf{q}}))\chi_{\kappa_1\mu_{2p}}^\dagger(\hat{\mathbf{p}})\chi_{\kappa_2\mu_{1s}}(\hat{\mathbf{p}}') \tag{74}$$

in a way to eliminate a dependence upon all angles except $\xi=\hat{\mathbf{p}}\cdot\hat{\mathbf{p}}'$. Summing over magnetic substates, we obtain

$$J=-\frac{1}{\sqrt{\pi}}\begin{Bmatrix} l_1 & l_2 & 1\\ \frac12 & \frac12 & \frac12\end{Bmatrix}\times\sum_M(-1)^M(\hat{p}\cdot\mathbf{Y}_{1LM}(\hat{\mathbf{q}}))Y_{l_1l_2}^{1-M}(\hat{\mathbf{p}},\hat{\mathbf{p}}') \tag{75}$$

$$=-\sqrt{\tfrac43}\begin{Bmatrix} l_1 & l_2 & 1\\ \frac12 & \frac12 & \frac12\end{Bmatrix}\sum_\sigma Y_{1\sigma}(\hat{\mathbf{p}})\times\sum_{Mm}(-1)^M C_{Lm,1\sigma}^{1M}Y_{Lm}(\hat{\mathbf{q}})Y_{l_1l_2}^{1-M}(\hat{\mathbf{p}},\hat{\mathbf{p}}'). \tag{76}$$

Here $Y_{l_1l_2}^{JM}$ is the bipolar spherical harmonic defined by Eq. (B7), $l_n=|\kappa_n+\frac12|-\frac12$, and $\{\cdots\}$ denotes a $6j$ symbol. After expanding $Y_{Lm}(\hat{\mathbf{q}})$ into a series of bipolar spherical harmonics according to Eq. (B12), expanding a product of bipolar spherical harmonics into the Clebsch-Gordon series according to Eq. (B10) and using the orthogonality condition for Clebsch-Gordon coefficients, we obtain

$$J=(-1)^{1+L}\sqrt{\tfrac43}\begin{Bmatrix} l_1 & l_2 & 1\\ \frac12 & \frac12 & \frac12\end{Bmatrix}\sum_{l_al_b}c_{l_al_b}^L\sum_{l_cl_d}B_{l_al_bL,l_1l_21}^{l_cl_d1}\times\sum_\sigma(-1)^\sigma Y_{1\sigma}(\hat{\mathbf{p}})Y_{l_cl_d}^{1-\sigma}(\hat{\mathbf{p}},\hat{\mathbf{p}}'). \tag{77}$$

The last sum can be evaluated to yield

$$\sum_\sigma(-1)^\sigma Y_{1\sigma}(\hat{\mathbf{p}})Y_{l_cl_d}^{1-\sigma}(\hat{\mathbf{p}},\hat{\mathbf{p}}')=\frac{3\sqrt{2l_c+1}}{(4\pi)^{3/2}}C_{l_c0,10}^{l_d0}(-1)^{l_c}P_{l_d}(\xi). \tag{78}$$

Using this and the explicit form of the coefficients $c_{l_1l_2}^L$ and $B_{l_1'l_2'L',l_1''l_2''L''}^{l_1l_2L}$ from Appendix B, we obtain

$$\sum_{\mu_{1s}\mu_{2p}M} s_{1M}^{2p1s}(\hat{\mathbf{p}}\cdot\mathbf{Y}_{10M}(\hat{\mathbf{q}}))\chi_{1\mu_{2p}}^\dagger(\hat{\mathbf{p}})\chi_{-1\mu_{1s}}(\hat{\mathbf{p}}')=-\frac{1}{8\pi^2}\frac{1}{\sqrt{2}}, \tag{79}$$

$$\sum_{\mu_{1s}\mu_{2p}M} s_{1M}^{2p1s}(\hat{\mathbf{p}}'\cdot\mathbf{Y}_{10M}(\hat{\mathbf{q}}))\chi_{1\mu_{2p}}^\dagger(\hat{\mathbf{p}})\chi_{-1\mu_{1s}}(\hat{\mathbf{p}}')=-\frac{1}{8\pi^2}\xi\frac{1}{\sqrt{2}}, \tag{80}$$

$$\sum_{\mu_{1s}\mu_{2p}M} s_{1M}^{2p1s}(\hat{\mathbf{p}}\cdot\mathbf{Y}_{12M}(\hat{\mathbf{q}}))\chi_{1\mu_{2p}}^\dagger(\hat{\mathbf{p}})\chi_{-1\mu_{1s}}(\hat{\mathbf{p}}')=\frac{1}{16\pi^2}\left[2-3p'^2\frac{1-\xi^2}{q^2}\right], \tag{81}$$

$$\sum_{\mu_{1s}\mu_{2p}M} s_{1M}^{2p1s}(\hat{\mathbf{p}}'\cdot\mathbf{Y}_{12M}(\hat{\mathbf{q}}))\chi_{1\mu_{2p}}^\dagger(\hat{\mathbf{p}})\chi_{-1\mu_{1s}}(\hat{\mathbf{p}}')=\frac{1}{16\pi^2}\left[2\xi-3pp'\frac{1-\xi^2}{q^2}\right]. \tag{82}$$

Now the angular integration in Eq. (72) is straightforward:

$$\Delta E_{34}=\frac{\alpha^2}{16\pi^5}\int_0^\infty dp\int_0^\infty dp'\int_{-1}^1 d\xi\,\frac{p^2p'^2}{q^2-\Delta_{2p1s}^2-i0}\times\left\{\frac{1}{\sqrt{2}}R_{10}^{2,1s2p}(q)[p\mathcal{R}_3^{2p1s}+\xi p'\mathcal{R}_4^{2p1s}]+\frac{1}{2}R_{12}^{2,1s2p}(q)\left[p\mathcal{R}_3^{2p1s}\left(2-3p'^2\frac{1-\xi^2}{q^2}\right)+p'\mathcal{R}_4^{2p1s}\left(2\xi-3pp'\frac{1-\xi^2}{q^2}\right)\right]\right\}. \tag{83}$$

Finally, we present the resulting formula for the exchange part of the free-vertex contribution for the $\delta E_{2p}^{(1s)}$ correction:

$$\Delta E_{\rm ver}^{(0),\rm exch}=\frac{\alpha^2}{16\pi^5}\int_0^\infty dp\int_0^\infty dp'\int_{-1}^1 d\xi\,\frac{p^2p'^2}{q^2-\Delta_{2p1s}^2-i0}\times\left\{R_1^{1,1s2p}(q)\left[\mathcal{F}_1^{2p1s}\frac{\xi p'-p}{q}-\mathcal{F}_2^{2p1s}\frac{\xi p-p'}{q}\right]+\frac{1}{\sqrt{2}}R_{10}^{2,1s2p}(q)[\xi\mathcal{R}_1^{2p1s}-3\mathcal{R}_2^{2p1s}+p\mathcal{R}_3^{2p1s}+\xi p'\mathcal{R}_4^{2p1s}+\xi p\mathcal{R}_5^{2p1s}+p'\mathcal{R}_6^{2p1s}]+\frac{1}{2}R_{12}^{2,1s2p}(q)\left[(-2\mathcal{R}_1^{2p1s}+p'\mathcal{R}_4^{2p1s}+p\mathcal{R}_5^{2p1s})\times\left(2\xi-3pp'\frac{1-\xi^2}{q^2}\right)+p\mathcal{R}_3^{2p1s}\left(2-3p'^2\frac{1-\xi^2}{q^2}\right)+p'\mathcal{R}_6^{2p1s}\left(2-3p^2\frac{1-\xi^2}{q^2}\right)\right]\right\}, \tag{84}$$

where expressions for the functions $\mathcal{F}_i^{ab}=\mathcal{F}_i^{ab}(p,p',\xi)$ and $\mathcal{R}_i^{ab}=\mathcal{R}_i^{ab}(p,p',\xi)$ are indicated in Appendix A.

B. $\Delta E_{\rm vr}^{\rm many}$ correction

The $\Delta E_{\rm vr}^{\rm many}$ correction is given by the sum of many-potential contributions of the vertex and the reducible term, as stated by Eq. (45). The many-potential part of the vertex term can be obtained by subtracting the contributions of the free-electron propagators from Eq. (24). For simplicity, we perform the angular integration and the summation over magnetic substates first and subtract the contribution of the free propagators in the final expression. The angular integration was evaluated by introducing the function $R_L(\omega,abcd)$ in the following way [19]:

$$4\pi\langle ab|\alpha_\mu\alpha_\nu D^{\mu\nu}(\omega)|cd\rangle=\sum_{J=0}^\infty I_J(abcd)R_J(\omega,abcd), \tag{85}$$

where the function $I_J(abcd)$ contains the whole dependence on magnetic quantum numbers,

$$I_J(abcd)=\sum_{m_J}(-1)^{j_a-m_a+J-m_J+j_b-m_b}\begin{pmatrix} j_a & J & j_c\\ -m_a & m_J & m_c\end{pmatrix}\times\begin{pmatrix} j_b & J & j_d\\ -m_b & -m_J & m_d\end{pmatrix}, \tag{86}$$

and $(\cdots)$ denotes a $3j$ symbol. The expression for the radial integral $R_J(\omega,abcd)$ is listed in Appendix C. Performing the summation over magnetic substates, we obtain

$$\Delta E_{\rm ver}=\frac{i\alpha^2}{2\pi}\sum_{n_1n_2}\int_{-\infty}^\infty d\omega\times\left\{\frac{S_1(\omega,n_1n_2)}{[\epsilon_v-\omega-\epsilon_{n_1}(1-i0)][\epsilon_v-\omega-\epsilon_{n_2}(1-i0)]}+\frac{S_2(\omega,n_1n_2)}{[\epsilon_c-\omega-\epsilon_{n_1}(1-i0)][\epsilon_c-\omega-\epsilon_{n_2}(1-i0)]}-2\frac{S_3(\omega,n_1n_2)}{[\epsilon_c-\omega-\epsilon_{n_1}(1-i0)][\epsilon_v-\omega-\epsilon_{n_2}(1-i0)]}\right\}, \tag{87}$$

where

$$S_1(\omega,n_1n_2)=\delta_{\kappa_1\kappa_2}\frac{(-1)^{j_1-1/2}}{\sqrt{2(2j_1+1)}}R_0(0,n_1cn_2c)\times\sum_L(-1)^LR_L(\omega,vn_2n_1v), \tag{88}$$

$$S_2(\omega,n_1n_2)=\delta_{\kappa_1\kappa_2}\frac{(-1)^{j_1-1/2}}{\sqrt{2(2j_1+1)}}R_0(0,vn_1vn_2)\times\sum_L(-1)^LR_L(\omega,cn_2n_1c), \tag{89}$$

$$S_3(\omega,n_1n_2)=\frac{(-1)^{j_1+j_2}}{2}\sum_{L_1L_2}\begin{Bmatrix}\frac{1}{2} & \frac{1}{2} & L_1\\ j_1 & j_2 & L_2\end{Bmatrix}\times R_{L_1}(\Delta_{vc},n_1vn_2c)R_{L_2}(\omega,cn_2n_1v), \tag{90}$$

and the summation in Eq. (87) is performed over Dirac angular-momentum quantum numbers and principal quantum numbers of intermediate states. To evaluate the double sum over the complete spectrum of the Dirac equation, we write Eq. (87) in terms of the Green function. To obtain the many-potential part, we subtract the contribution of free propagators. The resulting expression has a rather complicated structure. Thus we present the final expression only for the $\delta E_{2p}^{(1s)}$ correction:

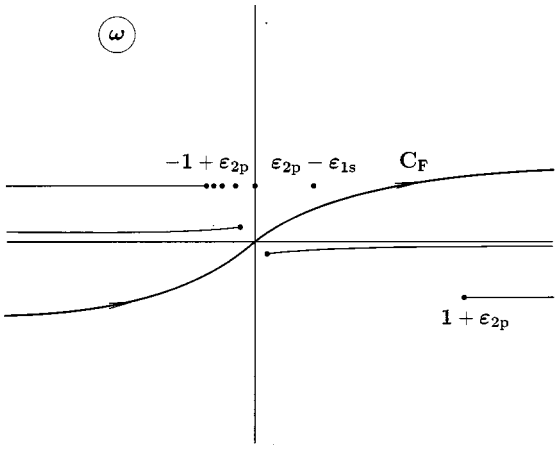

FIG. 4. The contour C_F of the ω integration in Eq. (91). The poles and the branch cuts shown are defined by the analytic properties of the Green functions and the photon propagator.

$$\Delta E_{\rm ver}^{\rm many}=\Delta E_{\rm ver}^{\rm infr}+\frac{i\alpha^2}{2\pi}\sum_{\kappa_1}\int_{C_F}d\omega\int_0^\infty dy_1\,dy_2\,dz\,y_1^2y_2^2z^2$$
$$\times\Bigg\{P_0^{1,1s1s}(z)[\mathbf{D}_{\kappa_1\kappa_1}(\epsilon_{2p},\epsilon_{2p})]^{\bar{l}_1}_{2p2p}+P_0^{1,2p2p}(z)$$
$$\times[\mathbf{D}_{\kappa_1\kappa_1}(\epsilon_{1s},\epsilon_{1s})]^{l_1}_{1s1s}-\sum_{\kappa_2}\sqrt{6}C_1(\kappa_1,\kappa_2)$$
$$\times\sum_J(-1)^{J+j_2+1/2}\begin{Bmatrix}\frac{1}{2}&\frac{1}{2}&1\\ j_1&j_2&J\end{Bmatrix}$$
$$\times[\mathbf{R}_{\kappa_1\kappa_2}(\varepsilon_{1s},\varepsilon_{2p})]_{1s2p}\Bigg\}, \tag{91}$$

where the contour C_F is indicated in Fig. 4 and

$$[\mathbf{D}_{\kappa_1\kappa_1}(\epsilon_a,\epsilon_a)]^l_{aa}=2|\kappa_1|g_l(\omega)\{\mathbf{D}_{\kappa_1\kappa_1}(\epsilon_a,\epsilon_a)\}^I_{aa}$$
$$-\sum_{JL}(2J+1)g_L(\omega)$$
$$\times\{\mathbf{D}_{\kappa_1\kappa_1}(\epsilon_a,\epsilon_a)\}^{II,aa}_{\kappa_1\kappa_1,JL}, \tag{92}$$

$$[\mathbf{R}_{\kappa_1\kappa_2}(\epsilon_{1s},\epsilon_{2p})]_{1s2p}=\delta_{Jl_1}(-1)^{j_1-j_2}2\sqrt{|\kappa_1\kappa_2|}g_{l_1}(\omega)$$
$$\times\{\mathbf{R}_{\kappa_1\kappa_2}(\epsilon_{1s},\epsilon_{2p})\}^I_{1s2p}$$
$$-\sum_L(2J+1)g_L(\omega)$$
$$\times\{\mathbf{R}_{\kappa_1,\kappa_2}(\epsilon_{1s},\epsilon_{2p})\}^{II,1s2p}_{\kappa_1\kappa_2,JL}, \tag{93}$$

$$\{\mathbf{A}\}^I_{ab}=g_a(y_1)A_{11}(y_1,z,y_2)g_b(y_2)$$
$$+g_a(y_1)A_{12}(y_1,z,y_2)f_b(y_2)$$
$$+f_a(y_1)A_{21}(y_1,z,y_2)g_b(y_2)$$
$$+f_a(y_1)A_{22}(y_1,z,y_2)f_b(y_2), \tag{94}$$

$$\{\mathbf{A}\}^{II,ab}_{\kappa_1\kappa_2,JL}=f_a(y_1)A_{11}(y_1,z,y_2)f_b(y_2)S_{JL}(-\kappa_a,\kappa_1)$$
$$\times S_{JL}(-\kappa_b,\kappa_2)-f_a(y_1)A_{12}(y_1,z,y_2)g_b(y_2)$$
$$\times S_{JL}(-\kappa_a,\kappa_1)S_{JL}(\kappa_b,-\kappa_2)$$
$$-g_a(y_1)A_{21}(y_1,z,y_2)f_b(y_2)S_{Jl}(\kappa_a,-\kappa_1)$$
$$\times S_{JL}(-\kappa_b,\kappa_2)+g_a(y_1)A_{22}(y_1,z,y_2)g_b(y_2)$$
$$\times S_{JL}(\kappa_a,-\kappa_1)S_{JL}(-\kappa_b,\kappa_2). \tag{95}$$

$\mathbf{D}_{\kappa_1\kappa_2}$ and $\mathbf{R}_{\kappa_1\kappa_2}$ are 2×2 matrices defined as follows:

$$\mathbf{R}_{\kappa_1\kappa_2}(\epsilon_a,\epsilon_b)=P_1^{1,ba}(z)\mathbf{D}_{\kappa_1\kappa_2}(\epsilon_a,\epsilon_b)$$
$$-\sum_{L=0,2}P_L^{2,ba}(z)\mathbf{Q}^L_{\kappa_1\kappa_2}(\epsilon_a,\epsilon_b), \tag{96}$$

$$\mathbf{D}_{\kappa_1\kappa_2}(\epsilon_a,\epsilon_b;y_1,z,y_2)$$
$$=\mathbf{G}_{\kappa_1}(\epsilon_a-\omega,y_1,z)\mathbf{G}_{\kappa_2}(\epsilon_b-\omega,z,y_2)$$
$$-\mathbf{G}^{(0)}_{\kappa_1}(\epsilon_a-\omega,y_1,z)\mathbf{G}^{(0)}_{\kappa_2}(\epsilon_b-\omega,z,y_2)$$
$$-\frac{1}{\omega^2}\varphi_a(y_1)\varphi_a^T(z)\varphi_b(z)\varphi_b^T(y_2), \tag{97}$$

$$\mathbf{Q}^L_{\kappa_1\kappa_2}(\epsilon_a,\epsilon_b;y_1,z,y_2)$$
$$=\mathbf{G}_{\kappa_1}(\epsilon_a-\omega,y_1,z)\mathbf{A}^L_{\kappa_1\kappa_2}\mathbf{G}_{\kappa_2}(\epsilon_b-\omega,z,y_2)$$
$$-\mathbf{G}^{(0)}_{\kappa_1}(\epsilon_a-\omega,y_1,z)\mathbf{A}^L_{\kappa_1\kappa_2}\mathbf{G}^{(0)}_{\kappa_2}(\epsilon_b-\omega,z,y_2)$$
$$-\frac{1}{\omega^2}\varphi_a(y_1)\varphi_a^T(z)\mathbf{A}^L_{\kappa_1\kappa_2}\varphi_b(z)\varphi_b^T(y_2). \tag{98}$$

Here $\mathbf{G}_\kappa(\omega,x_1,x_2)$ is the radial Green function of the Dirac equation (see Ref. [14] for details). $\mathbf{G}^{(0)}_\kappa(\omega,x_1,x_2)$ is the free Dirac Green function, $\varphi_n(x)$ denotes the radial wave function

$$\varphi_n(x)=\begin{pmatrix}g_n(x)\\ f_n(x)\end{pmatrix}, \tag{99}$$

and the matrices $\mathbf{A}^L_{\kappa_1\kappa_2}$ are given by

$$\mathbf{A}^0_{\kappa_1\kappa_2}=\begin{pmatrix}0&1\\-1&0\end{pmatrix}+(\kappa_2-\kappa_1)\begin{pmatrix}0&1\\1&0\end{pmatrix}, \tag{100}$$

$$\mathbf{A}^2_{\kappa_1\kappa_2}=-2\begin{pmatrix}0&1\\-1&0\end{pmatrix}+(\kappa_2-\kappa_1)\begin{pmatrix}0&1\\1&0\end{pmatrix}. \tag{101}$$

In Eqs. (97) and (98) we subtract the free-electron contribution and the singular infrared term from the contribution of the bound-electron propagators. The contribution of the infrared term is readded in Eq. (91) where it is denoted $\Delta E_{\rm ver}^{\rm infr}$. The other notations are $\bar{l}_n=2j_n-l_n$, $C_1(\kappa_1,\kappa_2)$ and $g_L(\omega)$ are defined by Eqs. (C10) and (C6), and the radial integrals $P_L^{i,ab}(z)$ are defined as

$$P_L^{1,ab}(x_2)=\int_0^\infty dx_1\, x_1^2 g_L(\Delta_{ab},x_<,x_>) \times[g_a(x_1)g_b(x_1)+f_a(x_1)f_b(x_1)], \quad (102)$$

$$P_0^{2,ab}(x_2)=\int_0^\infty dx_1\, x_1^2 g_0(\Delta_{ab},x_<,x_>) \times[\tfrac{1}{3}g_a(x_1)f_b(x_1)+f_a(x_1)g_b(x_1)], \quad (103)$$

$$P_2^{2,ab}(x_2)=\int_0^\infty dx_1\, x_1^2 g_2(\Delta_{ab},x_<,x_>)\tfrac{2}{3}g_a(x_1)f_b(x_1). \quad (104)$$

Note that in Eq. (91) only the summation over κ_1 is infinite. In all other sums only a few nonvanishing terms remain after taking into account the triangular selection rules of the Clebsch-Gordon coefficients.

The many-potential part of the reducible term can be evaluated in the same way:

$$\Delta E_{\rm red}^{B,\rm many}=\Delta E_{\rm red}^{\rm infr}+\frac{i\alpha^2}{2\pi}\sum_{\kappa_1}\int_{C_F}d\omega\int_0^\infty dy_1\,dy_2\,dz y_1^2 y_2^2 z^2 \times\left(-\frac{1}{2\alpha}\right)\Delta E_{1\rm ph}\{[\mathbf{D}_{\kappa_1\kappa_1}(\epsilon_{2p},\epsilon_{2p})]^{\bar{l}_1}_{2p2p} +[\mathbf{D}_{\kappa_1\kappa_1}(\epsilon_{1s},\epsilon_{1s})]^{l_1}_{1s1s}\}. \quad (105)$$

Here we refer to the singular infrared part of the expression as $\Delta E_{\rm red}^{\rm infr}$. The two infrared terms from the vertex and the reducible part should be calculated together to obtain a finite result. A straightforward calculation yields

$$\Delta E_{\rm red}^{\rm infr}+\Delta E_{\rm ver}^{\rm infr}=\frac{\alpha^2}{4\pi}R_1(\Delta_{2p1s},2p1s1s2p) \times\Big\{2\tilde{R}_0(1s2p1s2p)+\tfrac{2}{3}\tilde{R}_1(1s2p1s2p) -\sum_{L=0,1}(-1)^L[\tilde{R}_L(1s1s1s1s) +\tilde{R}_L(2p2p2p2p)]\Big\}, \quad (106)$$

where radial integrals $\tilde{R}_L(abcd)$ are defined analogously to $R_L(\omega,abcd)$ (see Appendix C), with the function $g_l(\omega,x_1,x_2)$ substituted by $\tilde{g}_l(x_1,x_2)$:

$$\tilde{g}_l(x_1,x_2)=\frac{1}{2l+2}[zQ_l(z)-Q_{l-1}(z)] \quad \text{for } l\neq 0, \quad (107)$$

$$\tilde{g}_l(x_1,x_2)=\tfrac{1}{2}[Q_1(z)+\ln|x_1^2-x_2^2|] \quad \text{for } l=0, \quad (108)$$

where $z=(x_1^2+x_2^2)/(2x_1x_2)$ and $Q_k(z)$ is the Legendre polynomial of second kind. The function $\tilde{g}_l(x_1,x_2)$ is the radial part of the partial-wave expansion of $\ln(|\mathbf{x}_{12}|)$. Note that in the separation and in the evaluation of the infrared contributions we assume the $2s$ and $2p_{1/2}$ Dirac levels to be nondegenerated, i.e., the finite nuclear-size effect should be taken into account in actual calculations.

C. $\Delta E_{\rm ir}$ and $\Delta E_{\rm red}^A$ corrections

Summing Eqs. (20)–(22) over magnetic substates of core electrons and performing the angular integration, we obtain the expression for the irreducible contribution:

$$\Delta E_{\rm ir}=2\{\langle c|\Sigma(\epsilon_c)|\xi_c\rangle+\langle v|\Sigma(\epsilon_v)|\xi_v\rangle\}, \quad (109)$$

$$|\xi_c\rangle=\alpha\sum_{\epsilon_n\neq\epsilon_c}\frac{|n\rangle}{\epsilon_c-\epsilon_n}\Big\{R_0(0,cvnv) -\sum_L\frac{(-1)^L}{2}R_L(\Delta_{vc},vcnv)\Big\}, \quad (110)$$

$$|\xi_v\rangle=\alpha\sum_{\epsilon_n\neq\epsilon_v}\frac{|n\rangle}{\epsilon_v-\epsilon_n}\Big\{R_0(0,cvcn) -\sum_L\frac{(-1)^L}{2}R_L(\Delta_{vc},vccn)\Big\}. \quad (111)$$

A simple calculation for the $\Delta E_{\rm red}^A$ correction yields

$$\Delta E_{\rm red}^A=\alpha\sum_L\frac{(-1)^L}{2}R_L'(\Delta_{vc},vccv) \times[\langle c|\Sigma(\epsilon_c)|c\rangle-\langle v|\Sigma(\epsilon_v)|v\rangle], \quad (112)$$

where $R_L'(\Delta_{vc})=(d/d\omega)R_L(\omega)|_{\omega=\Delta_{vc}}$.

III. NUMERICAL DETAILS AND RESULTS

For the calculation of the irreducible contribution we use the numerical procedure developed for the first-order self-energy correction and described in detail in Ref. [14]. We mention here only a few new features of the evaluation compared to [14]. The effective wave function $|\xi\rangle$ contains the sum over the whole spectrum of the Dirac equation except the initial state. The summation was performed using the method of the *B*-spline basis set for the Dirac equation [20]. The $|\xi\rangle$ function was stored on the radial grid and then obtained at an arbitrary point by interpolation. We note that, due to a presence of a nonzero imaginary part in the $|\xi\rangle$ function for the $\delta E_{2s}^{(1s)}$ and the $\delta E_{2p}^{(1s)}$ correction, the imaginary part of the self-energy operator yields a nonzero contribution to the real part of the irreducible contribution. Another new feature compared to [14] is that the calculation was performed for the shell model of the nuclear charge distribution. The Green function for the extended nucleus was evaluated in a way similar to the one used in Ref. [21]. Our computation of the Whittaker functions and their derivatives is discussed in detail in Ref. [14]. For the calculation of the zero- and the one-potential contribution one has to evaluate numerically the Fourier transform of wave functions. We start from the numerical coordinate-space wave function and evaluate the Fourier transform by a direct point-by-point numerical integration. For small values of momentum the Gauss-Legendre integration was used, and the generalized Clenshaw-Curtis algorithm was used otherwise. The wave

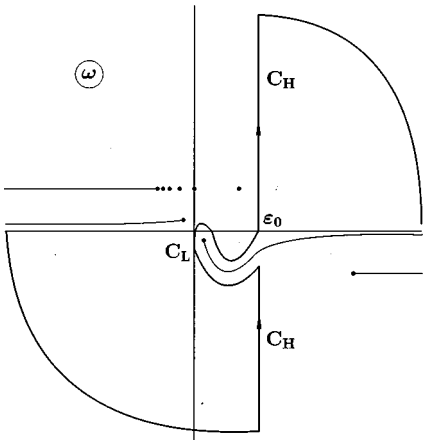

FIG. 5. The deformed contour of the ω integration in the many-potential vertex term. The contour is divided into two parts, C_L and C_H, which correspond to the low- and the high-energy part, respectively.

functions in momentum representation were stored on a grid and interpolated afterwards to obtain the value at an arbitrary point.

The computation of the free contributions is similar to the evaluation of the one-potential term for the first-order self-energy correction described in Ref. [14]. A new feature in the present case is that the photon propagator in momentum representation in Eq. (60) contains a singularity when $q^2=\Delta^2$. In the case $\Delta=0$, the singularity is integrable while for nonzero values of Δ the singularity should be treated according to the Feynman rules for bypassing of poles of the photon propagator. We have

$$\frac{1}{\Delta^2-q^2+i0}=\mathrm{P}\left(\frac{1}{\Delta^2-q^2}\right)-i\pi\delta(\Delta^2-q^2), \qquad (113)$$

where P denotes that the principal value of the integral should be taken. The second term in Eq. (113) contributes only to the imaginary part of the correction and can be omitted. The principal value of the integral was evaluated numerically using the transformation of variables $\{pp'\xi\}\to\{xyq\}$, where

$$x=p+p', \qquad (114)$$

$$y=p-p', \qquad (115)$$

$$q=\sqrt{p^2+p'^2-2pp'\xi}. \qquad (116)$$

The integral over q in a vicinity of the pole can be schematically represented to be

$$\mathrm{P}\int_{\Delta-a}^{\Delta+a}dq\,\frac{F(q)}{\Delta-q}, \qquad (117)$$

where $F(q)$ remains regular at $q=\Delta$. We evaluate the function $F(q)$ in several points within the interval $[\Delta-a,\Delta+a]$ and interpolate it by a polynomial. The principal value of the integral is then obtained analytically.

For the calculation of the many-potential contributions we deform the contour C_F of the ω integration in a way shown in Fig. 5 in analogy to the evaluation of the first-order self-energy correction in Ref. [14]. We divide the integral into two parts that correspond to integrations over two parts C_L and C_H of the new contour and refer to them as the *low-energy* and the *high-energy* terms, respectively. As a test of our code, we use also an alternative approach to the numerical evaluation of the many-potential contributions. In that approach, we rotate the integration contour C_F to the imaginary axis. All the pole contributions and singular terms were separated and calculated using the method of the *B*-spline basis set [20]. The comparison of these two approaches was used also to estimate the numerical uncertainty of the calculation. The numerical evaluation of the many-potential contributions is numerically the most intensive part of the computation. To reduce the computing time, a storage and a subsequent interpolation of different functions was widely used. So, we store for each $|\kappa|$ and ω all Whittaker and Bessel functions required for the computation of Green's functions. The radial integrals $P_L^{i,ab}$ in Eq. (91) and the wave functions of the initial states were stored as well. The summation over the absolute value of κ_1 in Eq. (91) and in Eq. (105) was performed after all the integrations were completed. The sum was terminated at $|\kappa_1|=20$ and the remainder was estimated using a polynomial fitting in $1/|\kappa_1|$.

The results of the calculation of the two-electron self-energy correction $\delta E_{2p}^{(1s)}$ due to the interaction of the electron in the $2p_{1/2}$ state and the $(1s)^2$ shell are given in Table I. Values of the rms radii used in the calculation [23–26] are listed in the second column of the table. In the next columns of Table I the various contributions to the $\delta E_{2p}^{(1s)}$ correction are listed. The results are presented in terms of the function $F(\alpha Z)$ defined by

$$\delta E=\alpha^2(\alpha Z)^3F(\alpha Z)mc^2. \qquad (118)$$

The total $\delta E_{2p}^{(1s)}$ correction is listed in the last two columns of Table I.

The calculation of the two-electron self-energy correction $\delta E_{2s}^{(1s)}$ due to the interaction of the electron in the $2s$ state and the $(1s)^2$ shell was performed in Ref. [10]. Here we recalculate this correction using the numerical scheme presented in this article, which differs slightly from the procedure used in Ref. [10]. Various contribution to the $\delta E_{2s}^{(1s)}$ correction are given in Table II.

The calculation of the two-electron self-energy correction δE_{1s}^{1s} due to the interaction of electrons in the $(1s)^2$ shell was performed in Refs. [8,9,22]. In Table III we present the various contributions to this correction. (The correction for thorium, given in [8], was recalculated with the new rms radius 5.802 fm [26].) These results perfectly agree with the ones from Ref. [22].

The total two-electron self-energy contributions to the $(1s)^22s$ and the $(1s)^22p_{1/2}$ state of Li-like ions are given by the sums $\delta E_{2s}^{(1s)}+\delta E_{1s}^{1s}$ and $\delta E_{2p}^{(1s)}+\delta E_{1s}^{1s}$, respectively.

IV. $2p_{1/2}$-$2s$ TRANSITION ENERGY IN Li-LIKE IONS

In Table IV we summarize all the contributions calculated up to now for the energy of the $2p_{1/2}$-$2s$ transition in Li-like ions. In the second column of the table the one-electron Dirac energy contributions are listed. The correction due to the one-photon exchange is given in the third column. These

TABLE I. Various contributions to the $\delta E_{2p}^{(1s)}$ correction due to the interaction of the electron in the $2p_{1/2}$ state and the $(1s)^2$ shell. The function $F(\alpha Z)$ is defined by Eq. (118).

Z	$\langle r^2\rangle^{1/2}$ (fm)	$F_{\rm ir}$	$F_{\rm vr}^{\rm free}$	$F_{\rm vr}^{\rm many}$	$F_{\rm red}^{A}$	$F_{2p}^{(1s)}$	$\delta E_{2p}^{(1s)}$ (eV)
18	3.427	−0.1003	1.7456	−1.7685	0.0010	−0.1221(15)	−0.007 53(9)
20	3.478	−0.0951	1.4089	−1.4311	0.0011	−0.1162(12)	−0.009 83(10)
30	3.928	−0.0803	0.6167	−0.6375	0.0019	−0.0992(4)	−0.028 33(10)
32	4.072	−0.0790	0.5406	−0.5614	0.0021	−0.0977(2)	−0.033 84(7)
40	4.270	−0.0776	0.3424	−0.3634	0.0028	−0.0959(2)	−0.064 90(13)
50	4.655	−0.0824	0.2151	−0.2378	0.0036	−0.1015(2)	−0.134 1(3)
54	4.787	−0.0860	0.1824	−0.2062	0.0040	−0.1059(2)	−0.176 3(3)
60	4.914	−0.0934	0.1444	−0.1703	0.0045	−0.1149(2)	−0.262 3(5)
66	5.224	−0.1032	0.1153	−0.1440	0.0050	−0.1270(2)	−0.386 2(7)
70	5.317	−0.1114	0.0993	−0.1303	0.0053	−0.1372(2)	−0.497 7(8)
74	5.373	−0.1212	0.0853	−0.1190	0.0056	−0.1493(2)	−0.639 7(9)
80	5.467	−0.1393	0.0668	−0.1055	0.0061	−0.1719(2)	−0.930 5(11)
83	5.533	−0.1504	0.0585	−0.1000	0.0063	−0.1855(2)	−1.121 8(12)
90	5.802	−0.1830	0.0402	−0.0899	0.0067	−0.2260(2)	−1.742 0(15)
92	5.860	−0.1946	0.0353	−0.0877	0.0069	−0.2402(2)	−1.977 4(17)
100	5.886	−0.2553	0.0148	−0.0812	0.0072	−0.3145(2)	−3.325 2(21)

corrections are calculated using the Fermi model of the nuclear charge distribution

$$\rho(r)=\frac{N}{1+\exp[(r-c)/a]} \tag{119}$$

with the rms radii listed in Table I. The parameter a is fixed to be $a=2.3/(4\ln 3)$ fm. The parameters c and N can be expressed with a good precision in terms of the rms radius by (see, e.g., Ref. [27])

$$c^2=\tfrac{5}{3}\langle r^2\rangle-\tfrac{7}{3}a^2\pi^2, \tag{120}$$

$$N=\frac{3}{4\pi c^3}\left(1+\frac{\pi^2a^2}{c^2}\right)^{-1}. \tag{121}$$

The uncertainty given in the first two columns for $Z<83$ is obtained by the one percent variation of the rms radius. For bismuth, thorium, and uranium the rms radius is known more precisely. In the case $Z=90$ [$\langle r^2\rangle^{1/2}=5.802(4)$ fm [26]] and $Z=92$ [$\langle r^2\rangle^{1/2}=5.860(2)$ fm [28]] the uncertainty is estimated by taking the difference between results obtained using the Fermi model and the homogeneously charged sphere model with the same rms radius. For $Z=83$, the uncertainty results from a variation of the rms radius by 0.020 fm (it corresponds to a discrepancy between two measured values [23]).

The one-electron self-energy correction and the Wichman-Kroll contribution to the one-electron vacuum-polarization correction are taken from recent tabulations [29,30]. The one-electron Uehling contribution is calculated using the Fermi model of the nuclear charge distribution.

TABLE II. Various contributions to the $\delta E_{2s}^{(1s)}$ correction due to the interaction of the electron in the $2s$ state and the $(1s)^2$ shell. The function $F(\alpha Z)$ is defined by Eq. (118).

Z	$F_{\rm ir}$	$F_{\rm vr}^{\rm free}$	$F_{\rm vr}^{\rm many}$	$F_{\rm red}^{A}$	$F_{2s}^{(1s)}$	$\delta E_{2s}^{(1s)}$ (eV)
18	−0.5168	1.9751	−2.0341	0.0003	−0.5754(6)	−0.035 49(4)
20	−0.4895	1.5838	−1.6411	0.0003	−0.5465(4)	−0.046 24(4)
30	−0.3970	0.6699	−0.7226	0.0006	−0.4491(2)	−0.128 21(6)
32	−0.3843	0.5831	−0.6353	0.0006	−0.4360(2)	−0.151 05(7)
40	−0.3461	0.3591	−0.4107	0.0009	−0.3967(2)	−0.268 49(14)
50	−0.3179	0.2189	−0.2714	0.0012	−0.3692(2)	−0.488 03(26)
54	−0.3112	0.1838	−0.2373	0.0014	−0.3633(2)	−0.604 88(34)
60	−0.3050	0.1438	−0.1994	0.0017	−0.3589(2)	−0.819 81(46)
66	−0.3033	0.1143	−0.1725	0.0019	−0.3596(2)	−1.093 2(6)
70	−0.3044	0.0985	−0.1591	0.0022	−0.3628(2)	−1.315 8(7)
74	−0.3075	0.0850	−0.1483	0.0024	−0.3684(2)	−1.578 3(9)
80	−0.3158	0.0682	−0.1362	0.0028	−0.3810(2)	−2.062 7(11)
83	−0.3218	0.0608	−0.1317	0.0030	−0.3896(2)	−2.355 3(12)
90	−0.3409	0.0457	−0.1244	0.0037	−0.4159(2)	−3.205 9(15)
92	−0.3479	0.0418	−0.1230	0.0039	−0.4253(2)	−3.501 7(16)
100	−0.3848	0.0270	−0.1209	0.0050	−0.4737(2)	−5.008 6(21)

TABLE III. Various contributions to the δE^{1s}_{1s} correction due to the interaction of the electrons in the $(1s)^2$ shell for Li-like ions. The function $F(\alpha Z)$ is defined by Eq. (118).

Z	$F_{\rm ir}$	$F^{\rm free}_{\rm vr}$	$F^{\rm many}_{\rm vr}$	F^{1s}_{1s}	δE^{1s}_{1s} (eV)
18	−1.4367	2.8137	−3.1864	−1.8094(3)	−0.111 59(2)
20	−1.3579	2.2064	−2.5621	−1.7135(3)	−0.144 95(3)
30	−1.0907	0.8186	−1.1167	−1.3887(2)	−0.396 49(6)
32	−1.0543	0.6909	−0.9812	−1.3446(2)	−0.465 89(7)
40	−0.9435	0.3675	−0.6352	−1.2112(2)	−0.819 69(14)
50	−0.8605	0.1711	−0.4240	−1.1134(2)	−1.471 7(3)
54	−0.8398	0.1227	−0.3728	−1.0899(2)	−1.814 7(3)
60	−0.8193	0.0678	−0.3164	−1.0679(2)	−2.439 2(5)
66	−0.8103	0.0267	−0.2767	−1.0603(2)	−3.223 5(6)
70	−0.8103	0.0043	−0.2568	−1.0628(2)	−3.854 8(7)
74	−0.8151	−0.0152	−0.2410	−1.0712(2)	−4.590 1(9)
80	−0.8313	−0.0408	−0.2230	−1.0951(2)	−5.928 9(11)
83	−0.8437	−0.0525	−0.2162	−1.1124(2)	−6.725 6(12)
90	−0.8848	−0.0782	−0.2046	−1.1676(2)	−9.000 9(15)
92	−0.9002	−0.0853	−0.2023	−1.1878(2)	−9.780 0(17)
100	−0.9819	−0.1143	−0.1967	−1.2929(2)	−13.671 7(21)

There is not yet any QED calculation of the two-photon exchange diagrams for the transition considered here. Thus we employ results of many-body calculations [3–7] to obtain an approximation to the correction due to exchange by two or more photons. This correction is listed in Table IV in the sixth column. We found that results of different many-body calculations are in a good agreement with each other; thus, we use mainly the extensive tabulation of Kim *et al.* [3].

The error estimates assigned to the results of many-body calculations originate predominantly from their incomplete treatment of the two-photon exchange correction. Only for small Z we include into the uncertainty also a discrepancy between different calculations. We would like to stress that there is no well-defined way to estimate a QED contribution to the two-photon exchange, which is omitted in many-body calculations. The second-order Breit-interaction contribution, which arises in many-body calculations, cannot be used for a meaningful error estimation since it contributes only in the order $\alpha^2(\alpha Z)^4$ while the leading order of QED correction is known to be $\alpha^2(\alpha Z)^3$. The uncertainty given in the table should be considered to give only an order of magnitude of the QED correction.

The two-electron self-energy correction is calculated in this paper and the two-electron vacuum-polarization contribution is taken from Ref. [11]. The nuclear recoil correction was calculated by Artemyev *et al.* [31], the nuclear polariza-

TABLE IV. Various contributions to the $2p_{1/2}$-$2s$ transition energy in Li-like ions (in eV).

			One-electron			Two-electron				
Z	Extended nucleus	One-photon exchange	Self-energy	Vacuum polarization	⩾Two-photon exchange	Self-energy	Vacuum polarization	Nuclear recoil	Nuclear polarization	Total
18	−0.001	35.570	−0.168	0.011	−3.564(3)	0.028	−0.002	−0.009		31.865(3)
20	−0.002	39.769	−0.242	0.016	−3.604(3)	0.036	−0.002	−0.012		35.960(3)
28	−0.010	57.455	−0.779	0.062	−3.841(5)	0.084	−0.006	−0.015		52.950(5)
30	−0.014	62.147	−0.989	0.082	−3.919(6)	0.100	−0.008	−0.016		57.383(6)
32	−0.021	66.967	−1.237	0.107	−4.004(8)	0.117	−0.010	−0.016		61.904(8)
40	−0.07	87.76	−2.68	0.27	−4.42(2)	0.20	−0.02	−0.02		81.03(2)
47	−0.18	108.43	−4.69	0.52	−4.90(3)	0.30	−0.03	−0.02		99.43(3)
50	−0.27	118.17	−5.83	0.68	−5.15(3)	0.35	−0.04	−0.03		107.90(3)
54	−0.44(1)	132.11	−7.64	0.95	−5.51(4)	0.43	−0.05	−0.03		119.82(4)
60	−0.89(2)	155.44	−11.11	1.52	−6.15(6)	0.56	−0.07	−0.03		139.26(6)
66	−1.87(3)	182.31	−15.68	2.36	−6.94(10)	0.71	−0.11	−0.03		160.75(10)
70	−2.92(5)	202.61	−19.45	3.12	−7.56(13)	0.82	−0.13	−0.04		176.46(14)
74	−4.49(8)	225.21	−23.92	4.09	−8.27(20)	0.94	−0.16	−0.04		193.35(22)
80	−8.59(14)	264.30(1)	−32.16	6.07	−9.55(20)	1.13	−0.21	−0.05		220.95(24)
83	−11.94(7)	286.68	−37.08	7.36	−10.30(30)	1.23	−0.25	−0.05		235.65(31)
90	−26.63(5)	348.29	−51.11	11.43	−12.44(40)	1.46	−0.33	−0.07	0.02	270.64(40)
92	−33.35(6)	368.83	−55.87	12.94	−13.20(40)	1.52	−0.36	−0.07	0.03	280.49(40)

TABLE V. Comparision between various theoretical calculations and experimental results for the $2p_{1/2}$-$2s$ transition energy in Li-like ions (in eV).

Z	This paper	Blundell (Ref. [4])	Chen *et al.* (Ref. [7])	Persson *et al.* (Ref. [36])	Expt.	Reference
18	31.865(3)	31.868(1)			31.866(1)	Edlén, Ref. [37]
20	35.960(3)	35.964(1)	35.963		35.962(2)	Sugar and Corliss, Ref. [38]
28	52.950(5)				52.950(2)	Hinnov and Denne, Ref. [39]
					52.950(1)	Sugar *et al.*, Ref. [40]
					52.947(4)	Staude *et al.*, Ref. [41]
30	57.383(6)	57.389(2)			57.384(3)	Staude *et al.*, Ref. [41]
32	61.904(8)	61.911(2)	61.907		61.902(4)	Hinnov and Denne, Ref. [39]
					61.901(2)	Knize, Ref. [42]
40	81.03(2)	81.04				
47	99.43(3)				99.438(7)	Bosselmann *et al.*, Ref. [43]
50	107.90(3)	107.92(1)				
54	119.82(4)	119.84(1)	119.82		119.97(10)	Martin *et al.*, Ref. [44]
					119.820(8)	Bosselmann, Ref. [45]
60	139.26(6)	139.29(1)				
70	176.46(14)	176.56(2)				
80	220.95(24)	220.99(3)				
90	270.64(40)	270.72(5)	270.80			
92	280.49(40)	280.83(10)	280.74	280.59(15)	280.59(9)	Schweppe *et al.*, Ref. [1]

tion correction for thorium and uranium was calculated by Plunien and Soff [32] and by Nefiodov *et al.* [33].

The second-order one-electron QED corrections are not yet completely calculated and, therefore, they are not included in the table. The present status of these calculations can be found in Ref. [34]. The calculation of the two-loop self-energy correction, which may yield a dominant α^2 one-electron contribution, is still in progress [35]. We expect the whole second-order one-electron QED contribution to yield a few tenths of eV for uranium.

In Table V the comparison of the present calculations with previous theoretical and experimental results is given. One can see that the experimental accuracy obtained for Li-like ions in a wide range of Z is high enough to test QED contributions beyond the lowest-order Lamb shift. To achieve the level of the experimental accuracy in theoretical predictions for very high Z, rigorous calculations of the two-photon exchange diagrams and the two-loop one-electron self-energy are needed. The first correction is likely to be calculated in the near future [46]. After calculations of all QED corrections of order α^2 are finished, the accuracy of the theoretical predictions will be limited mainly by the uncertainty of the effect of the extended nuclear charge distribution. In the case of uranium, this uncertainty is slightly less than the experimental error, if the currently accepted value of the rms radius $[\langle r^2\rangle^{1/2}=5.860(2)$ fm [28]] is used. However, a one percent deviation of the rms radius alters the total Lamb shift value by 0.5 eV.

ACKNOWLEDGMENTS

We are grateful to Ph. Bosselmann and his co-workers for making their results available to us prior to publication. The work of V.A.Y., A.N.A, and V.M.S. was supported by the Russian Foundation for Basic Research (Grant No. 98-02-18350) and by the program ''Russian Universities Basis Research'' (Project No. 3930). G.S. and G.P. acknowledge support by the BMBF, GSI, and DFG. T.B. is grateful for support by the EU-TMR program under Contract No. ERB FMRX CT 97-0144.

APPENDIX A: FREE-VERTEX OPERATOR

The free-electron vertex operator in the Feynman gauge reads

$$\Gamma^{\mu}(\mathrm{p},\mathrm{p}')=-4\pi i\alpha\int\frac{d^4\mathrm{k}}{(2\pi)^4}\frac{1}{\mathrm{k}^2}\gamma_{\sigma}\times\frac{\not{\mathrm{p}}-\not{\mathrm{k}}+m}{(\mathrm{p}-\mathrm{k})^2-m^2}\gamma^{\mu}\frac{\not{\mathrm{p}}'-\not{\mathrm{k}}+m}{(\mathrm{p}'-\mathrm{k})^2-m^2}\gamma^{\sigma}. \quad \text{(A1)}$$

We separate the ultraviolet divergence in $\Gamma^{\mu}(\mathrm{p},\mathrm{p}')$ using dimensional regularization with $D=4-2\epsilon$:

$$\Gamma^{\mu}(\mathrm{p},\mathrm{p}')=\frac{\alpha}{4\pi}\Delta_{\epsilon}\gamma^{\mu}+\Gamma^{\mu}_{R}(\mathrm{p},\mathrm{p}'), \quad \text{(A2)}$$

where $\Delta_{\epsilon}=1/\epsilon-\gamma_E+\ln 4\pi-\ln m^2$.

When considering the free-vertex correction, one has to evaluate the expression $\overline{\psi}_a(\mathbf{p})\Gamma^{\mu}_{R}(\mathrm{p},\mathrm{p}')\big|_{\substack{\mathbf{p}^0=\epsilon_a\\ \mathbf{p}'^0=\epsilon_b}}\psi_b(\mathbf{p}')$. To perform the angular integration, it is convenient to write this expression in the form $[\Gamma^{\mu}_{R}=(\Gamma^0_R,\mathbf{\Gamma}_R)]$:

$$\overline{\psi}_a(\mathbf{p})\Gamma^0_R(\mathrm{p},\mathrm{p}')\psi_b(\mathbf{p}')=\frac{\alpha}{4\pi}i^{l_a-l_b}\{\mathcal{F}_1^{ab}\chi^{\dagger}_{\kappa_a\mu_a}(\hat{\mathbf{p}})\chi_{\kappa_b\mu_b}(\hat{\mathbf{p}}')+\mathcal{F}_2^{ab}\chi^{\dagger}_{-\kappa_a\mu_a}(\hat{\mathbf{p}})\chi_{-\kappa_b\mu_b}(\hat{\mathbf{p}}')\}, \quad \text{(A3)}$$

$$\overline{\psi}_a(\mathbf{p})\mathbf{\Gamma}_R(\mathrm{p},\mathrm{p}')\psi_b(\mathbf{p}')$$
$$= \frac{\alpha}{4\pi} i^{l_a-l_b}\{\mathcal{R}_1^{ab}\chi^\dagger_{\kappa_a\mu_a}(\hat{\mathbf{p}})\boldsymbol{\sigma}\chi_{-\kappa_b\mu_b}(\hat{\mathbf{p}}')$$
$$+\mathcal{R}_2^{ab}\chi^\dagger_{-\kappa_a\mu_a}(\hat{\mathbf{p}})\boldsymbol{\sigma}\chi_{\kappa_b\mu_b}(\hat{\mathbf{p}}')$$
$$+(\mathcal{R}_3^{ab}\mathbf{p}+\mathcal{R}_4^{ab}\mathbf{p}')\chi^\dagger_{\kappa_a\mu_a}(\hat{\mathbf{p}})\chi_{\kappa_b\mu_b}(\hat{\mathbf{p}}')$$
$$+(\mathcal{R}_5^{ab}\mathbf{p}+\mathcal{R}_6^{ab}\mathbf{p}')\chi^\dagger_{-\kappa_a\mu_a}(\hat{\mathbf{p}})\chi_{-\kappa_b\mu_b}(\hat{\mathbf{p}}')\}, \tag{A4}$$

where

$$\mathcal{F}_1^{ab}(p,p',\xi)=A\tilde{g}_a\tilde{g}'_b+(B_1\epsilon_a+B_2\epsilon_b)(\epsilon_a\tilde{g}_a+p\tilde{f}_a)\tilde{g}'_b$$
$$+(C_1\epsilon_a+C_2\epsilon_b)\tilde{g}_a(\epsilon_b\tilde{g}'_b+p'\tilde{f}'_b)$$
$$+D(\epsilon_a\tilde{g}_a+p\tilde{f}_a)(\epsilon_b\tilde{g}'_b+p'\tilde{f}'_b)$$
$$+(H_1\epsilon_a+H_2\epsilon_b)\tilde{g}_a\tilde{g}'_b, \tag{A5}$$

$$\mathcal{F}_2^{ab}(p,p',\xi)=A\tilde{f}_a\tilde{f}'_b+(B_1\epsilon_a+B_2\epsilon_b)(\epsilon_a\tilde{f}_a+p\tilde{g}_a)\tilde{f}'_b$$
$$+(C_1\epsilon_a+C_2\epsilon_b)\tilde{f}_a(\epsilon_b\tilde{f}'_b+p'\tilde{g}'_b)$$
$$+D(\epsilon_a\tilde{f}_a+p\tilde{g}_a)(\epsilon_b\tilde{f}'_b+p'\tilde{g}'_b)$$
$$-(H_1\epsilon_a+H_2\epsilon_b)\tilde{f}_a\tilde{f}'_b, \tag{A6}$$

$$\mathcal{R}_1^{ab}(p,p',\xi)=A\tilde{g}_a\tilde{f}'_b-D(\epsilon_a\tilde{g}_a+p\tilde{f}_a)(\epsilon_b\tilde{f}'_b+p'\tilde{g}'_b), \tag{A7}$$

$$\mathcal{R}_2^{ab}(p,p',\xi)=A\tilde{f}_a\tilde{g}'_b-D(\epsilon_a\tilde{f}_a+p\tilde{g}_a)(\epsilon_b\tilde{g}'_b+p'\tilde{f}'_b), \tag{A8}$$

$$\mathcal{R}_3^{ab}(p,p',\xi)=B_1(\epsilon_a\tilde{g}_a+p\tilde{f}_a)\tilde{g}'_b+C_1\tilde{g}_a(\epsilon_b\tilde{g}'_b+p'\tilde{f}'_b)$$
$$+H_1\tilde{g}_a\tilde{g}'_b, \tag{A9}$$

$$\mathcal{R}_4^{ab}(p,p',\xi)=B_2(\epsilon_a\tilde{g}_a+p\tilde{f}_a)\tilde{g}'_b+C_2\tilde{g}_a(\epsilon_b\tilde{g}'_b+p'\tilde{f}'_b)$$
$$+H_2\tilde{g}_a\tilde{g}'_b, \tag{A10}$$

$$\mathcal{R}_5^{ab}(p,p',\xi)=B_1(\epsilon_a\tilde{f}_a+p\tilde{g}_a)\tilde{f}'_b+C_1\tilde{f}_a(\epsilon_b\tilde{f}'_b+p'\tilde{g}'_b)$$
$$-H_1\tilde{f}_a\tilde{f}'_b, \tag{A11}$$

$$\mathcal{R}_6^{ab}(p,p',\xi)=B_2(\epsilon_a\tilde{f}_a+p\tilde{g}_a)\tilde{f}'_b+C_2\tilde{f}_a(\epsilon_b\tilde{f}'_b+p'\tilde{g}'_b)$$
$$-H_2\tilde{f}_a\tilde{f}'_b, \tag{A12}$$

where $\mathrm{p}=(\epsilon_a,\mathbf{p})$, $\mathrm{p}'=(\epsilon_b,\mathbf{p}')$, $p=|\mathbf{p}|$, $p'=|\mathbf{p}'|$, $\xi=\hat{\mathbf{p}}\cdot\hat{\mathbf{p}}'$, $l_n=|\kappa_n+\frac{1}{2}|-\frac{1}{2}$, and $\tilde{g}$ and $\tilde{f}$ denote the components of the wave function in momentum representation $\tilde{g}_n=\tilde{g}_n(p)$, $\tilde{f}_n=\tilde{f}_n(p)$, $\tilde{g}'_n=\tilde{g}_n(p')$, $\tilde{f}'_n=\tilde{f}_n(p')$. The functions A, $B_{1,2}$, $C_{1,2}$, D, and $H_{1,2}$ are defined in Appendix B of Ref. [14]. [We note that in Ref. [14] the free-vertex operator is defined in the form $\Gamma^\mu(\mathrm{p}',\mathrm{p})$. Thus p and p' have to be interchanged in the expressions therein.]

APPENDIX B: VECTOR AND BIPOLAR SPHERICAL HARMONICS

In this section we collect some basic formulas for the evaluation of angular integrals in coordinate and momentum space.

The evaluation of corrections with the scalar part of the photon propagator leads to the basic angular integrals that can be easily calculated to be

$$\int d\hat{\mathbf{z}}\,\chi^\dagger_{\kappa_b\mu_b}(\hat{\mathbf{z}})Y_{LM}(\hat{\mathbf{z}})\chi_{\kappa_a\mu_a}(\hat{\mathbf{z}})=s^{ba}_{LM}C_L(\kappa_b,\kappa_a), \tag{B1}$$

where

$$s^{ba}_{LM}=\left(\frac{2L+1}{4\pi}\right)^{1/2}(-1)^{j_b-\mu_b}\begin{pmatrix} j_b & L & j_a \\ -\mu_b & M & \mu_a\end{pmatrix}. \tag{B2}$$

The coefficients $C_L(\kappa_b,\kappa_b)$ are defined by Eq. (C10).

When considering corrections with the vector part of the photon propagator, one encounters the expression

$$\chi^\dagger_{\kappa_b\mu_b}(\hat{\mathbf{z}})\boldsymbol{\sigma}\chi_{\kappa_a\mu_a}(\hat{\mathbf{z}}). \tag{B3}$$

To perform the angular integration, we expand this expression in terms of vector spherical harmonics [19]:

$$\chi^\dagger_{\kappa_b\mu_b}(\hat{\mathbf{z}})\boldsymbol{\sigma}\chi_{\kappa_a\mu_a}(\hat{\mathbf{z}})=\sum_{JLM}s^{ab}_{JM}S_{JL}(\kappa_b,\kappa_a)\mathbf{Y}_{JLM}(\hat{\mathbf{z}}), \tag{B4}$$

where the coefficients $S_{JL}(\kappa_b,\kappa_b)$ are defined by Eqs. (C7)–(C9). Vector spherical harmonics $\mathbf{Y}_{JLM}(\hat{\mathbf{z}})$ are defined in the following way:

$$\mathbf{Y}_{JLM}(\hat{\mathbf{z}})=\sum_{mq}C^{JM}_{Lm,1q}Y_{Lm}(\hat{\mathbf{z}})\mathbf{e}_q, \tag{B5}$$

where $\mathbf{e}_q$ are the spherical coordinates of the unit vector. Vector spherical harmonics obey the orthogonality condition

$$\int d\hat{\mathbf{z}}\,\mathbf{Y}^\dagger_{JLM}(\hat{\mathbf{z}})\mathbf{Y}_{J'L'M'}(\hat{\mathbf{z}})=\delta_{JJ'}\delta_{LL'}\delta_{MM'}. \tag{B6}$$

For the evaluation of the exchange part of the free-vertex correction, we use bipolar spherical harmonics defined by [47]

$$Y^{JM}_{l_1l_2}(\hat{\mathbf{z}}_1,\hat{\mathbf{z}}_2)=\sum_{m_1m_2} C^{JM}_{l_1m_1,l_2m_2}Y_{l_1m_1}(\hat{\mathbf{z}}_1)Y_{l_2m_2}(\hat{\mathbf{z}}_2). \tag{B7}$$

For the important special case $J=0$ a bipolar harmonic is reduced to

$$Y^{00}_{l_1l_2}(\hat{\mathbf{z}}_1,\hat{\mathbf{z}}_2)=\delta_{l_1l_2}(-1)^{l_1}\frac{\sqrt{2l_1+1}}{4\pi}P_{l_1}(\xi), \tag{B8}$$

where $\xi=\hat{\mathbf{z}}_1\cdot\hat{\mathbf{z}}_2$. Bipolar spherical harmonics obey the orthogonality condition

$$\int d\hat{\mathbf{z}}_1\,d\hat{\mathbf{z}}_2\,Y^{JM\dagger}_{l_1l_2}(\hat{\mathbf{z}}_1,\hat{\mathbf{z}}_2)Y^{J'M'}_{l_1'l_2'}(\hat{\mathbf{z}}_1,\hat{\mathbf{z}}_2)=\delta_{JJ'}\delta_{MM'}\delta_{l_1l_1'}\delta_{l_2l_2'}. \tag{B9}$$

A useful expansion of a product of two bipolar spherical harmonics reads [47]

$$Y^{L'M'}_{l_1'l_2'}(\hat{\mathbf{z}}_1,\hat{\mathbf{z}}_2)Y^{L''M''}_{l_1''l_2''}(\hat{\mathbf{z}}_1,\hat{\mathbf{z}}_2)=\sum_{LM} C^{LM}_{L'M',L''M''}\sum_{l_1l_2} B^{l_1l_2L}_{l_1'l_2'L',l_1''l_2''L''}Y^{LM}_{l_1l_2}(\hat{\mathbf{z}}_1,\hat{\mathbf{z}}_2), \tag{B10}$$

where

$$B^{l_1l_2L}_{l_1'l_2'L',l_1''l_2''L''}=\left(\frac{(2l_1'+1)(2l_2'+1)(2l_1''+1)(2l_2''+1)(2L'+1)(2L''+1)}{(4\pi)^2}\right)^{1/2}C^{l_10}_{l_1'0,l_1''0}C^{l_20}_{l_2'0,l_2''0}\begin{Bmatrix} l_1' & l_1'' & l_1\\ l_2' & l_2'' & l_2\\ L' & L'' & L\end{Bmatrix} \tag{B11}$$

and $\{\cdots\}$ denotes a $9j$ symbol. The spherical harmonics can be expanded into a series of bipolar spherical harmonics as [47]

$$Y_{LM}(\hat{\mathbf{z}})=\sum_{\substack{l_1,l_2=0\\ l_1+l_2=L}}^{L} c^L_{l_1l_2}Y^{LM}_{l_1l_2}(\hat{\mathbf{z}}_1,\hat{\mathbf{z}}_2), \tag{B12}$$

where $\mathbf{z}=\mathbf{z}_1-\mathbf{z}_2$ and

$$c^L_{l_1l_2}=\left(\frac{4\pi(2L+1)!}{(2l_1+1)!(2l_2+1)!}\right)^{1/2}\frac{z_1^{l_1}z_2^{l_2}}{z^L}. \tag{B13}$$

APPENDIX C: RADIAL INTEGRAL $R_J(\omega,abcd)$

The evaluation of the radial integral $R_J(\omega,abcd)$ defined by Eq. (85) can be found in [19]. For our purposes it is convenient to write it in the form

$$\begin{aligned}R_J(\omega,abcd)&=(2J+1)\int_0^\infty x_2^2\,dx_2\,x_1^2\,dx_1\\&\times\Big\{(-1)^J C_J(\kappa_a,\kappa_c)C_J(\kappa_b,\kappa_d)\\&\times g_J(\omega,x_<,x_>)W_{ac}(x_1)W_{bd}(x_2)\\&-\sum_L(-1)^L g_L(\omega,x_<,x_>)X_{ac}(x_1)X_{bd}(x_2)\Big\},\end{aligned} \tag{C1}$$

$$W_{ab}(x)=g_a(x)g_b(x)+f_a(x)f_b(x), \tag{C2}$$

$$\begin{aligned}X_{ab}(x)=&g_a(x)f_b(x)S_{JL}(-\kappa_b,\kappa_a)\\&-f_a(x)g_b(x)S_{JL}(\kappa_b,-\kappa_a),\end{aligned} \tag{C3}$$

where g_n,f_n are the upper and the lower radial components of the Dirac wave function, respectively, $x_>=\max(x_1,x_2)$, $x_<=\min(x_1,x_2)$. The function $g_l(\omega,x_<,x_>)$ is the radial part of the partial wave expansion of the photon propagator,

$$\frac{e^{i\omega|\mathbf{x}_{12}|}}{|\mathbf{x}_{12}|}=\sum_l(2l+1)g_l(\omega,x_<x_>)P_l(\xi), \tag{C4}$$

$$g_l(0,x_<x_>)=\frac{1}{2l+1}\frac{x_<^l}{x_>^{l+1}}, \tag{C5}$$

$$g_l(\omega,x_<x_>)=i\omega j_l(\omega x_<)h_l^{(1)}(\omega x_>), \tag{C6}$$

where $P_l(z)$ is the Legendre polynomial and $j_l(z),h_l^{(1)}(z)$ are the spherical Bessel functions, $\xi=\hat{\mathbf{x}}_1\cdot\hat{\mathbf{x}}_2$.

The angular coefficients $S_{JL}(\kappa_a,\kappa_b)$ differ from zero only for $L=J$, $J\pm1$ and can be written for $J\neq0$ as

$$S_{JJ+1}(\kappa_a,\kappa_b)=\left(\frac{J+1}{2J+1}\right)^{1/2}\left(1+\frac{\kappa_a+\kappa_b}{J+1}\right)C_j(-\kappa_b,\kappa_a), \tag{C7}$$

$$S_{JJ}(\kappa_a,\kappa_b)=\frac{\kappa_a-\kappa_b}{\sqrt{J(J+1)}}C_J(\kappa_b,\kappa_a), \tag{C8}$$

$$S_{JJ-1}(\kappa_a,\kappa_b)=\left(\frac{J}{2J+1}\right)^{1/2}\left(-1+\frac{\kappa_a+\kappa_b}{J}\right)C_J(-\kappa_b,\kappa_a). \tag{C9}$$

In the case $J=0$ there is only one nonvanishing coefficient $S_{01}(\kappa_a,\kappa_b)=C_0(-\kappa_b,\kappa_a)$.

The coefficients $C_J(\kappa_b,\kappa_a)$ are given by

$$C_J(\kappa_b,\kappa_a)=(-1)^{j_b+1/2}\sqrt{(2j_a+1)(2j_b+1)}\times\begin{pmatrix} j_a & J & j_b \\ \frac{1}{2} & 0 & -\frac{1}{2}\end{pmatrix}\Pi(l_a,l_b,J), \tag{C10}$$

where the symbol $\Pi(l_a,l_b,J)$ is unity if l_a+l_b+J is even, and zero otherwise.

[1] J. Schweppe, A. Belkacem, L. Blumenfeld, N. Claytor, B. Feinberg, H. Gould, V. E. Kostroun, L. Levy, S. Misawa, J. R. Mowat, and M. H. Prior, Phys. Rev. Lett. **66**, 1434 (1991).

[2] P. Beiersdorfer, A. Osterheld, J. Scofield, J. Crespo Lopez-Urrutia, and K. Widmann, Phys. Rev. Lett. **80**, 3022 (1998).

[3] Y.-K. Kim, D. H. Baik, P. Indelicato, and J. P. Desclaux, Phys. Rev. A **44**, 148 (1991).

[4] S. Blundell, Phys. Rev. A **47**, 1790 (1993).

[5] A. Ynnerman, J. James, I. Lindgren, H. Persson, and S. Salomonson, Phys. Rev. A **50**, 4671 (1994).

[6] P. Indelicato and J. P. Desclaux, Phys. Rev. A **42**, 5139 (1990).

[7] M. H. Chen, K. T. Cheng, W. R. Johnson, and J. Sapirstein, Phys. Rev. A **52**, 266 (1995).

[8] V. A. Yerokhin, A. N. Artemyev, and V. M. Shabaev, Phys. Lett. A **234**, 361 (1997).

[9] H. Persson, S. Salomonson, P. Sunnergren, and I. Lindgren, Phys. Rev. Lett. **76**, 204 (1996).

[10] V. A. Yerokhin, A. N. Artemyev, T. Beier, V. M. Shabaev, and G. Soff, J. Phys. B **31**, L691 (1998).

[11] A. N. Artemyev, T. Beier, G. Plunien, V. M. Shabaev, G. Soff, and V. A. Yerokhin, Phys. Rev. A **60**, 45 (1999).

[12] V. A. Yerokhin, A. N. Artemyev, T. Beier, V. M. Shabaev, and G. Soff, Phys. Scr. T **80**, 495 (1999).

[13] V. M. Shabaev, A. N. Artemyev, and V. A. Yerokhin, in *Trapped Charged Particles and Fundamental Physics*, edited by D. H. E. Dubin and D. Schneider (AIP, New York, 1998), p. 22.

[14] V. A. Yerokhin and V. M. Shabaev, Phys. Rev. A **60**, 800 (1999).

[15] V. M. Shabaev, Sov. Phys. J. **33**, 660 (1990).

[16] V. M. Shabaev and I. G. Fokeeva, Phys. Rev. A **49**, 4489 (1994).

[17] V. M. Shabaev, Phys. Rev. A **50**, 4521 (1994).

[18] E. M. Rose, *Relativistic Electron Theory* (Wiley, New York, 1961).

[19] W. R. Johnson, S. A. Blundell, and J. Sapirstein, Phys. Rev. A **37**, 2764 (1988).

[20] W. R. Johnson, S. A. Blundell, and J. Sapirstein, Phys. Rev. A **37**, 307 (1988).

[21] G. Soff and P. Mohr, Phys. Rev. A **38**, 5066 (1988).

[22] P. Sunnergren, Ph.D. thesis, Göteborg University and Chalmers University of Technology, Göteborg, 1998.

[23] G. Fricke, C. Bernhardt, K. Heilig, L. A. Schaller, L. Schellenberg, E. B. Shera, and C. W. de Jager, At. Data Nucl. Data Tables **60**, 177 (1995).

[24] H. de Vries, C. W. de Jager, and C. de Vries, At. Data Nucl. Data Tables **36**, 495 (1987).

[25] W. R. Johnson and G. Soff, At. Data Nucl. Data Tables **33**, 405 (1985).

[26] J. D. Zumbro, R. A. Naumann, M. V. Hoehn, W. Reuter, E. B. Shera, C. E. Bemis, Jr., and Y. Tanaka, Phys. Lett. **167B**, 383 (1986).

[27] V. M. Shabaev, J. Phys. B **26**, 1103 (1993).

[28] J. D. Zumbro, E. B. Shera, Y. Tanaka, C. E. Bemis, Jr., R. A. Naumann, M. V. Hoehn, W. Reuter, and R. M. Steffen, Phys. Rev. Lett. **53**, 1888 (1984).

[29] T. Beier, P. J. Mohr, H. Persson, and G. Soff, Phys. Rev. A **58**, 954 (1998).

[30] T. Beier, G. Plunien, M. Greiner, and G. Soff, J. Phys. B **30**, 2761 (1998).

[31] A. N. Artemyev, V. M. Shabaev, and V. A. Yerokhin, Phys. Rev. A **52**, 1884 (1995).

[32] G. Plunien and G. Soff, Phys. Rev. A **51**, 1119 (1995); **53**, 4614 (1996).

[33] A. V. Nefiodov, L. N. Labzowsky, G. Plunien, and G. Soff, Phys. Lett. A **222**, 227 (1996).

[34] P. J. Mohr, G. Plunien, and G. Soff, Phys. Rep. **293**, 227 (1998).

[35] S. Mallampalli and J. Sapirstein, Phys. Rev. A **57**, 1548 (1998).

[36] H. Persson, I. Lindgren, L. N. Labzowsky, G. Plunien, T. Beier, and G. Soff, Phys. Rev. A **54**, 2805 (1996).

[37] B. Edlén, Phys. Scr. **28**, 51 (1983).

[38] J. Sugar and C. Corliss, J. Phys. Chem. Ref. Data **14**, Suppl. No. 2 (1985).

[39] H. Hinnov and B. Denne, Phys. Rev. A **40**, 4357 (1989).

[40] J. Sugar, V. Kaufman, and W. L. Rowan, J. Opt. Soc. Am. B **9**, 344 (1992); **10**, 13 (1993).

[41] U. Staude, Ph. Bosselman, R. Büttner, D. Horn, K.-H. Schartner, F. Folkmann, A. E. Livingston, T. Ludziejewski, and P. H. Mokler, Phys. Rev. A **58**, 3516 (1998).

[42] R. J. Knize, Phys. Rev. A **43**, 1637 (1991).

[43] Ph. Bosselmann, U. Staude, D. Horn, K.-H. Schartner, F. Folkmann, A. E. Livingston, and P. H. Mokler, Phys. Rev. A **59**, 1874 (1999).

[44] S. Martin, J. P. Buchet, M. C. Buchet-Poulizac, A. Denis, J. Desesquelles, M. Druetta, J. P. Grandin, D. Hennecart, X. Husson, and D. Leclerc, Europhys. Lett. **10**, 645 (1989).

[45] Ph. Bosselmann, Ph.D. thesis, University of Gießen, Germany, 1999.

[46] J. Sapirstein, in *Trapped Charged Particles and Fundamental Physics* (Ref. [13]), p. 3.

[47] D. A. Varshalovich, A. N. Moskalev, and V. K. Khersonskii, *Quantum Theory of Angular Momentum* (World Scientific, Singapore, 1988).